Optical and Infrared Spectroscopy of SN 1999ee and SN 1999ex [1]

Mario Hamuy[2,3]

The Observatories of the Carnegie Institution of Washington, 813 Santa Barbara Street, Pasadena, CA 91101

mhamuy@ociw.edu

José Maza[3] [4]

Departamento de Astronomía, Universidad de Chile, Casilla 36-D, Santiago, Chile

jose@das.uchile.cl

Philip A. Pinto

Steward Observatory, The University of Arizona, Tucson, AZ 85721

ppinto@as.arizona.edu

M. M. Phillips

Carnegie Institution of Washington, Las Campanas Observatory, Casilla 601, La Serena, Chile

mmp@lco.cl

Nicholas B. Suntzeff

National Optical Astronomy Observatories[5], Cerro Tololo Inter-American Observatory, Casilla 603, La Serena, Chile

nsuntzeff@noao.edu

R. D. Blum

National Optical Astronomy Observatories[5], Cerro Tololo Inter-American Observatory, Casilla 603, La Serena, Chile

rblum@noao.edu

K.A.G. Olsen

National Optical Astronomy Observatories[5], Cerro Tololo Inter-American Observatory, Casilla 603, La Serena, Chile

kolsen@noao.edu

David J. Pinfield[3]

Astrophysics Research Institute, Liverpool John Moores University, Twelve Quays House, Egerton Wharf, Birkenhead, CH41 1LD, UK

dpi@astro.livjm.ac.uk

Valentin D. Ivanov

European Southern Observatory, Alonso de Córdova 3107, Vitacura, Casilla 19001, Santiago 19, Chile

vivanov@eso.org

T. Augusteijn[6]

European Southern Observatory, Alonso de Córdova 3107, Vitacura, Casilla 19001, Santiago 19, Chile

tau@ing.iac.es

S. Brillant

European Southern Observatory, Alonso de Córdova 3107, Vitacura, Casilla 19001, Santiago 19, Chile

sbrillan@eso.org

M. Chadid

European Southern Observatory, Alonso de Córdova 3107, Vitacura, Casilla 19001, Santiago 19, Chile

mchadid@eso.org

J.-G. Cuby

European Southern Observatory, Alonso de Córdova 3107, Vitacura, Casilla 19001, Santiago 19, Chile

jcuby@eso.org

V. Doublier

European Southern Observatory, Alonso de Córdova 3107, Vitacura, Casilla 19001, Santiago 19, Chile

vdoublie@eso.org

O. R. Hainaut

European Southern Observatory, Alonso de Córdova 3107, Vitacura, Casilla 19001, Santiago 19, Chile

ohainaut@eso.org

E. Le Floc'h

European Southern Observatory, Alonso de Córdova 3107, Vitacura, Casilla 19001, Santiago 19, Chile

elefloch@eso.org

C. Lidman

European Southern Observatory, Alonso de Córdova 3107, Vitacura, Casilla 19001, Santiago 19, Chile

clidman@eso.org

Monika G. Petr-Gotzens[7]

European Southern Observatory, Alonso de Córdova 3107, Vitacura, Casilla 19001, Santiago 19, Chile

mpetr@mpifr-bonn.mpg.de

E. Pompei

European Southern Observatory, Alonso de Córdova 3107, Vitacura, Casilla 19001, Santiago 19, Chile

epompei@eso.org

L. Vanzi

European Southern Observatory, Alonso de Córdova 3107, Vitacura, Casilla 19001, Santiago 19, Chile

lvanzi@eso.org

ABSTRACT

We report optical and infrared spectroscopic observations of the Type Ia SN 1999ee and the Type Ib/c SN 1999ex, both of which were hosted by the galaxy IC 5179. For SN 1999ee we obtained a continuous sequence with an unprecedented wavelength and temporal coverage beginning 9 days before maximum light and extending through day 42. Before maximum light SN 1999ee displayed a normal spectrum with a strong Si II λ6355 absorption, thus showing that not all slow-declining SNe are spectroscopically peculiar at these evolutionary phases. A comparative study of the infrared spectra of SN 1999ee and other Type Ia supernovae shows that there is a remarkable homogeneity among the Branch-normal SNe Ia during their first 60 days of evolution. SN 1991bg-like objects, on the other hand, display spectroscopic peculiarities at IR wavelengths. SN 1999ex was characterized by the lack of hydrogen lines, weak optical He I lines, and strong He I $\lambda\lambda$10830,20581, thus providing an example of an intermediate case between pure Ib and Ic supernovae. We conclude therefore that SN 1999ex provides first clear evidence for a link between the Ib and Ic classes and that there is a continuous spectroscopic sequence ranging from the He deficient SNe Ic to the SNe Ib which are characterized by strong optical He I lines.

Subject headings: supernovae

1. Introduction

The last ten years have witnessed an enormous progress in our knowledge of the optical properties of supernovae (SNe) of all types. However, comparatively little is still known about these objects in near-infrared (NIR) wavelengths. Given the rapid technological development of NIR light detection over recent years, in 1999 we started a program to obtain optical and NIR photometry

---

[1]Based on observations collected at the European Southern Observatory, Chile (program ESO 164.H-0376).

[2]Hubble Fellow

[3]Visiting Astronomer, European Southern Observatory.

[4]Visiting Astronomer, Cerro Tololo Inter-American Observatory. CTIO is operated by AURA, Inc. under contract to the National Science Foundation.

[5]Cerro Tololo Inter-American Observatory, Kitt Peak National Observatory, National Optical Astronomy Observatories, operated by the Association of Universities for Research in Astronomy, Inc., (AURA), under cooperative agreement with the National Science Foundation.

[6]Present address: Isaac Newton Group of Telescopes, Apartado de Correos 321, 38700 Santa Cruz de La Palma, Canary Islands, Spain

[7]Present address: Max-Planck-Institut für Radioastronomie, Auf dem Hügel 69, D-53121 Bonn, Germany

and spectroscopy of nearby SNe (z<0.08). So far, the "Supernova Optical and Infrared Survey" (SOIRS) program has gathered high-quality observations for ∼20 SNe. So far we have reported results for the bright Type II SN 1999em (Hamuy et al. 2001). In this paper we report spectroscopic observations of two of the best-observed objects included in our program, the Type Ia SN 1999ee and the Type Ib/c SN 1999ex, both of which exploded in the same galaxy within three weeks.

SN 1999ee was discovered by M. Wischnjewsky on a film taken on 1999 October 7.15 (JD 2451458.65) in the course of the El Roble survey (Maza & Hamuy 1999). The SN exploded 10 arcsec East and 10 arcsec South of the nucleus of the spiral galaxy IC 5179, a very active star-forming galaxy with a heliocentric redshift of 3,498 km s^{-1}. The optical spectrum taken on 1999 October 9.10 revealed the defining Si II λ6355 feature of the Type Ia class (Maza & Hamuy 1999). The high expansion velocity of 15,700 km s^{-1} deduced from this line and the faint apparent magnitude at discovery (∼17.5) indicated that this object had been found several days before maximum light. At the distance of the host galaxy SN 1999ee offered the promise to reach V=14.5 about 10 days later, thus proving to be an excellent target for a detailed study of a SN Ia early since explosion, both at optical and IR wavelengths. This discovery occurred at the very beginning of one of the SOIRS follow-up runs, previously scheduled for 1999 October-November, so we decided to give first priority to SN 1999ee. The unique opportunity afforded by SN 1999ee led the ESO Director General to allocate director's discretionary time to this project in order to secure the best possible data for SN 1999ee. As a result of this effort we obtained a superb dataset of optical/IR photometric and spectroscopic observations of the first 50 days of the evolution of SN 1999ee.

Three weeks after the discovery of SN 1999ee, a second SN exploded in the same galaxy that hosted SN 1999ee. The discovery of SN 1999ex was made by Martin et al. (1999) on 1999 November 9.51 UT (JD 2451492.01) in the course of the PARG Automated Supernova Search at Perth Observatory. They reported that the SN was not visible in a deep exposure taken on 1999 October 25.58 (estimated limiting mag 19), and that the object was slowly brightening. A spectrum taken on 1999 November 14.13 (Hamuy & Phillips 1999) showed that SN 1999ex had close resemblance to that of the Type Ic SN 1994I taken near maximum light (Filippenko et al. 1995). This led us initially to classify SN 1999ex as a Ic event although we believe that it should be typed as an intermediate Ib/c object (see Sec. 4.2). As soon as this object was discovered we decided to include it in our optical/IR spectroscopic follow-up.

The observations gathered for SNe 1999ee and 1999ex have an unprecedented temporal and wavelength coverage and afford the possibility to carry out a detailed comparison with atmosphere models. In this paper we report the spectroscopic observations of SNe 1999ee and 1999ex and we discuss these results. The spectra presented here are available in electronic form to other researchers (contact M. H. if interested). Optical and IR photometry will be published and discussed in detail elsewhere by Stritzinger et al. (2002) and Krisciunas et al. (2002), respectively.

2. Spectroscopic Observations and Reductions

We obtained optical and IR spectra of SNe 1999ee and 1999ex with the ESO NTT/EMMI/SOFI, the Danish 1.5-m/DFOSC equipments at La Silla, and the VLT/ISAAC instrument at Cerro Paranal between 1999 October 9 and 1999 November 28. We also obtained three optical spectra with the CTIO 4-m telescope on 1999 October 9, the CTIO 1.5-m telescope on 1999 October 27, and the Las Campanas Dupont 2.5-m telescope on 1999 October 16. Table 1 gives the journal of the observations.

2.1. Optical Spectroscopy

The NTT observations comprised three different setups. We used the blue channel of EMMI equipped with a Tek CCD (1024x1024) and grating 5 (158 lines mm^{-1}) which, in first order, delivered spectra with a dispersion of 3.5 Å pix^{-1} and a useful wavelength range between 0.330 and 0.525 μm. With the red channel, CCD Tek 2048, and grating 13 (150 lines mm^{-1}) the dispersion was 2.7 Å pix^{-1} and the spectral coverage included from 0.470 through 1.100 μm in first order. Since this setup had potential second-order contamination beyond $\sim$0.6 μm we decided to take one spectrum with the OG530 filter and a second observation without the filter, in order to provide an overlap with the blue spectrum. Thus, a single-epoch observation comprised three spectra.

The observations with EMMI started with calibrations during day time (bias and dome flat-field exposures). The night began with the observation of a spectrophotometric standard (from the list of Hamuy et al. (1994)) through a wide slit of 10 arcsec, after which we observed the SNe with a slit of 1 arcsec. Before the discovery of SN 1999ex on 1999 November 9 we oriented the slit along the line connecting SN 1999ee and the host galaxy nucleus. On 1999 November 14 and 19, on the other hand, we oriented the slit along the two SNe in order to get simultaneous spectra. Since the airmass of our observations was always below 1.5 we do not expect serious systematic errors in the observed fluxes due to atmospheric refraction. We took two exposures of the SNe per spectral setup, each of the same length (typically 300-600 sec). Immediately following this observation we observed a He-Ar lamp, at the same position of the SNe and before changing the optical setup in order to ensure an accurate wavelength calibration. At the end of the night we observed a second flux standard.

We also used the Danish 1.5-m telescope and the DFOSC instrument at La Silla on five nights, between 1999 October 20 and November 28, in order to improve the temporal coverage of our spectroscopic observations. In all cases we employed a 2K×2K LORAL CCD and two different grisms to secure a spectral coverage comparable to that obtained with EMMI. With grism 3 (400 lines mm^{-1}) we covered a useful wavelength range between 0.33 and 0.66 μm with a dispersion of 2.3 Å pix^{-1}. With grism 5 (300 lines mm^{-1}) we sampled the range between 0.53 and 0.98 μm at 3.1 Å pix^{-1}. The red setup produced spectra with significant fringing beyond 0.75 μm which we did not attempt to remove. We observed the SNe with a slit of 2 arcsec. Although we did not

rotate the slit along the parallactic angle, we obtained the first four spectra with airmass <1.1. The last spectrum taken on 1999 November 28, on the other hand, might suffer from atmospheric refraction since we obtained it with an airmass between 1.4-2.0. We took two 1200 sec exposures of the SNe per grism, followed by a He-Ne arc lamp exposure, and spectra of a flux standard with a 5 arcsec slit.

We obtained a spectrum of SN 1999ee on 1999 October 9 (two days after discovery) with the R-C spectrograph of the CTIO 4-m telescope, a 3K×1K LORAL CCD, and grating KPGL-2 (316 lines mm^{-1}) in first order. We took one 1800 sec exposure of the SN (through thick cirrus) with a 1.5 arcsec slit oriented along the parallactic angle, a He-Ar lamp exposure, and spectra of three flux standards through a 10 arcsec slit. The resulting SN spectrum had a dispersion of 1.9 Å pix^{-1} and useful wavelength coverage of 0.33-0.87 μm. Second-order contamination was expected beyond 0.66 μm since we did not include a blocking filter in the optical path. We obtained another spectrum at CTIO with the 1.5-m telescope and the R-C spectrograph on 1999 October 27. In this case we used a 1200×800 LORAL CCD, grating 58 (400 lines mm^{-1}) in second order, a 2 arcsec slit, and a $CuSO_4$ order-blocking filter. The resulting spectrum had a dispersion of 1.1 Å pix^{-1} and useful wavelength coverage of 0.37-0.50 μm. We obtained six 1200 sec exposures of SN 1999ee at an airmass < 1.1, a He-Ar lamp image, and two spectra of flux standards.

We also obtained a spectrum of SN 1999ee on 1999 October 16 with the Las Campanas Dupont 2.5-m telescope and the Wide Field CCD Spectrograph. We used a 2048×2048 TEK CCD and a blue grism. The resulting spectrum had a dispersion of 3 Å pix^{-1} and useful wavelength coverage of 0.36-0.92 μm. Second-order contamination was expected beyond 0.66 μm since we did not use a blocking filter.

The reductions consisted in subtracting the overscan and bias from every frame. Next, we constructed a normalized flat-field from the quartz-lamp image, duly normalized along the dispersion axis. We proceeded by flat-fielding all of the object frames and extracting 1-D spectra from the 2-D images. We followed the same procedure for the He-Ar frames which we used to derive the wavelength calibration for the SNe. Then we derived a response curve from the two flux stars, which we applied to the SN spectra, in order to get flux calibrated spectra. From the pair of flux-calibrated spectra that we obtained for each spectral setup we removed cosmic rays and obtained a clean spectrum of each SN. The last step consisted in merging the spectra obtained with the different spectroscopic setups. To avoid discontinuities in the combined spectrum we grey-shifted the three spectra relative to each other using the overlap regions. Finally, we computed the synthetic V-band magnitude from the resulting spectra (following the precepts described in Appendix B of Hamuy et al. (2001)) and we grey-shifted them so that the flux level matched our observed V magnitudes. We checked the spectrophotometric quality of the spectra by computing BRI synthetic magnitudes and comparing them to the observed BRI magnitudes of Stritzinger et al. (2002). Excluding the spectra obtained on 1999 November 14, this test yielded the following mean differences: B_{obs}-B_{syn}=-0.05±0.05, R_{obs}-R_{syn}=0.00±0.07, and I_{obs}-I_{syn}=0.00±0.09, which implies that the relative spectrophotometry at these wavelengths is accurate to 10% or better. The November

14 spectrum, on the other hand, shows B fluxes that fall 0.35 mag lower than the photometric B magnitudes and I fluxes that exceed by 0.2 mag the observed broadband I magnitudes, perhaps owing to atmospheric refraction effects.

2.2. Infrared Spectroscopy

We obtained five IR spectra with the VLT/Antu telescope at Cerro Paranal, between 1999 October 9 and November 28 (see Table 1). We employed the IR spectro-imager ISAAC (Moorwood 1997) in low resolution mode (R$\sim$500), with four different gratings that permitted us to obtain spectra in the SZ, J, H, and K bands. We used these gratings in 5^{th}, 4^{th}, 3^{rd} and 2^{nd} order, respectively, which yielded useful data in the spectral ranges 0.984-1.136, 1.109-1.355, 1.415-1.818, and 1.846-2.560 μm. The light detector was a Hawaii-Rockwell 1024x1024 array.

A typical IR observation started during daytime by taking calibrations. We began taking flat-field images using an internal source of continuum light. We obtained multiple on and off image pairs with the same slit used during the night (0.6 arcsec). We then took Xe-Ar lamp images (with the lamp on and off) with a narrow slit (0.3 arcsec) in order to map geometric distortions. The observations of the SNe consisted in an ABBAAB cycle, where A is an image of the SNe offset by 70 arcsec along the slit relative to the B image. This technique of nodding the objects along the slit allowed us to use the A image as an on-source observation and the B image as the off-source sky frame, and viceversa. At each position we exposed for 240 sec, conveniently split into two 120-sec images in order to remove cosmic rays and bad pixels from the final spectra. After completing the ABBAAB cycle we immediately obtained a pair of on-off arc lamp exposures without moving the telescope or changing optical elements to ensure an accurate wavelength calibration. We then switched to the next grating and repeated the above object-arc procedure until completing the observations with the four setups. For flux calibration we decided to observe a bright solar-analog star, close in the sky to the SNe in order to minimize variations in the atmospheric absorptions (Maiolino et al. 1996). The selected star was Hip 109508, of spectral type G3V, V=8.0, B-V=0.59, and located only 3° from the SNe. In this case we took two AB pairs for each grating. To avoid saturating the detector, we took the shortest possible exposures (1.77 sec) allowed by the electronics that controlled the detector. Since the minimum time required before offsetting the telescope was $\sim$60 sec, we took ten exposures at each position which provided an exceedingly good signal-to-noise ratio (S/N) for the flux standard.

Our data reduction procedures were explained in detail by Hamuy et al. (2001), so we include here only a brief summary. After dividing all of the object images by a normalized flat-field, we performed a first-order sky subtraction by subtracting the A images from the B exposures (and viceversa). We then shifted the A-B image relative to the B-A image in the spatial direction until matching the two spectra, and we added the shifted A-B image to the B-A image so that the resulting frame lacked any sky background, except for the pixel-to-pixel fluctuations expected from photon statistics and readout noise. We then extracted 1-D spectra of the objects from the

sky-subtracted frames, making sure to subtract residual DC offset and galaxy light from a window adjacent to the object. For flux calibration we adopted the technique described by Maiolino et al. (1996), which consists in dividing the spectrum of interest by a solar-type star to remove the strong telluric IR features, and multiplying the resulting spectrum by the solar spectrum to eliminate the intrinsic features (pseudonoise) introduced by the solar-type star. Before using the solar spectrum we convolved it with a kernel function in order to reproduce the spectral resolution of the solar-analog standard Hip 109508, we shifted it in wavelength according to the radial velocity (68 km s^{-1}) of Hip 109508, and we scaled it down to the equivalent of V=8.0 which corresponds to the observed magnitude of Hip 109508. This technique worked very well to remove telluric lines. On the other hand, it introduced a small systematic error in the flux calibration of the SN due to departures between the solar spectrum and the actual spectral energy distribution of the solar-analog standard. According to atmosphere models the difference in continuum flux for stars with T_{eff}=5,500 and 6,000 K (which correspond to spectral types G8V-F9V, Gray & Corbally (1994)) is smaller than 10% in the NIR region. A G3V star like Hip 109508 has nearly the same spectral type of the Sun, so its effective temperature must be close (within ±100 K) to that of the adopted solar model. Hence, the flux difference between the solar-analog standard and the adopted spectrum should be less than 10%. The $B-V$=0.59 color of Hip 109508 suggests little or no reddening so the relative spectrophotometry is probably accurate to 5% or better.

The result of these operations were four spectra covering the SZ, J, H, and K bands, which we combined into one final IR spectrum for each SN. Given the significant overlap of the SZ and J band spectra, we were able to grey-shift the J spectrum relative to the SZ spectrum. Then we used our broad-band JHK magnitudes to grey-shift the individual spectra.

On six occasions we used the NTT/SOFI instrument at La Silla in service observing mode, in order to complement the IR spectroscopic follow-up. We employed a Hawaii-Rockwell 1024x1024 light detector, and the blue and red grisms that permitted us to obtain spectra in the ranges 0.95-1.64 μm and 1.53-2.52 μm, with resolutions of 7.0 and 10.2 Å, respectively. We obtained the spectra with slit widths between 0.6 and 1 arcsec. We nodded the objects along the slit, after exposing for 150 sec at each position. We completed several pairs of AB observations for the SNe, we took Xe-Ne arc images at the position of the targets, and we observed the flux standard Hip 109508. We reduced these data following the same procedure explained above for ISAAC. The large overlap of 1.53-1.64 μm between the blue and red spectra allowed us to grey-shift the red spectra relative to blue spectra, except on 1999 October 18 when we were only able to obtain the red spectrum. Finally, we shifted the resulting spectra using the observed JHK magnitudes (Krisciunas et al. 2002).

3. Results

3.1. SN 1999ee

Before analyzing the spectroscopic observations it proves necessary to mention the photometric properties of SN 1999ee. A detailed discussion of the photometric observations can be found in Stritzinger et al. (2002). In brief, the decline rate of $\Delta m_{15}(B)$=0.94 puts SN 1999ee in the group of slowest-declining SNe Ia. After correcting the observed magnitudes for K terms and dust extinction, and assuming a Hubble constant of 63 km s^{-1} Mpc^{-1} (Phillips et al. 1999), SN 1999ee had a peak visual magnitude of M_V=-19.94 (JD 2451469.1). These values lie comfortably well with the peak magnitude-decline rate relation for SNe Ia (Phillips et al. 1999). This analysis reveals that SN 1999ee was a luminous Type Ia event and a very interesting object to check the claim by Li et al. (2001b) that slow-declining events display spectroscopic peculiarities before maximum light.

Figure 1 displays the optical spectra of SN 1999ee in the rest-frame of the SN, after correcting the observed spectra for the 3,498 km s^{-1} recession velocity of the host galaxy. We also dereddened the spectra assuming a Galactic reddening of $E(B-V)$=0.02 (Schlegel et al. 1998), and a host galaxy reddening of $E(B-V)$=0.30 derived from the SN optical colors (Stritzinger et al. 2002) and optical/IR colors (Krisciunas et al. 2002). The strongest telluric lines are indicated with the $\oplus$ symbol. The first spectrum, taken on JD 2451460.56 (9 days before maximum), exhibited a blue continuum and the characteristic P-Cygni profile of the Si II λ6355 line of SNe Ia. Other prominent features in this spectrum were the absorption at $\sim$3200 Å attributed to Co II, the Ca II H&K $\lambda\lambda$3934,3968 blend, Mg II λ4481, the blend of lines attributed to Fe II, Si II, S II around 4550-5050 Å , and the Ca II $\lambda\lambda$8498,8542,8662 triplet. The presence of the Na I D $\lambda\lambda$5890,5896, Ca II λ3934, and Ca II λ3968 interstellar lines with equivalent widths of 2.3, 0.8, and 0.6 Å, respectively, revealed a non-negligible amount of absorption in the host galaxy, which agrees with the color analysis of SN 1999ee. By maximum light the "W" shaped S II $\lambda\lambda$5454,5640 feature was well developed and the Ca lines were significantly stronger. Si II λ4129 was already present although it was quite weak. The Si II λ5972 line also was weak relative to Si II λ6355. Nugent et al. (1995) defined the parameter $\mathcal{R}$(Si II) as the relative fluxes of this pair of lines and found a tight correlation with the SN luminosity. In this case we obtained $\mathcal{R}$(Si II)=0.23 which corresponds to the value of a luminous SNe Ia, in good concordance with the decline rate of $\Delta m_{15}(B)$=0.94 and the peak magnitudes derived from the photometric observations. By day 20 the spectrum was much redder. The Si II λ6355 line was very weak, the Ca triplet had a pronounced P-Cygni profile, and the region between 4000-5500 Å was dominated by strong features due to Fe II transitions. The absorption attributed to Na I D $\lambda\lambda$5890,5896 was very prominent. Overall, these data showed that SN 1999ee was a genuine Type Ia event with the usual spectral features of other normal SNe Ia, usually known as Branch-normal (Branch et al. 1993).

Figure 2 presents the expansion velocities derived from the absorption minima of Si II λ6355, after correcting for the recession velocity of the host galaxy. Apparently the velocity derived from Si II λ6355 decreased rapidly from 16,000 to 10,000 km s^{-1} between days -7 and -2, after which

the velocity decreased slowly. For comparison we include as solid line the velocities for SN 1990N which was also caught several days before maximum (Leibundgut et al. 1991). Both SNe showed an inflection in the velocity curve. Before maximum, however, the expansion of SN 1999ee was somewhat higher compared to contemporary velocities of SN 1990N. At maximum light and later times, on the other hand, both SNe had similar velocities.

Figure 3 shows the resulting rest-frame IR spectra of SN 1999ee. The first spectrum, taken nine days before maximum, was quite featureless. A weak absorption line could be seen at 10520 Å with a weak emission component that seemed to constitute a P-Cygni profile. This feature was observed for the first time in an early-time spectrum of SN 1994D and was tentatively identified as due to either He I λ10830 or Mg II λ10926 (Meikle et al. 1996). According to the atmosphere models computed by Wheeler et al. (1998), this feature should be due to Mg II since the amount of He in their models is not sufficient to form a line. This implies that the minimum of the Mg absorption had an expansion velocity of 11,100 km s^{-1}. An emission due to Fe III (Rudy et al. 2002) was also present around 12550 Å. There was an indication of a P-Cygni profile with the absorption minimum at 16160 Å and peak emission at 16840 Å . This feature was also present in the SN 1994D spectrum. The theoretical modeling of Wheeler et al. suggests that this line is due to Si II, although it might have a Fe II component (Axelrod 1980). At longer wavelengths the spectrum is even more featureless except for a small P-Cygni line with a minimum at 19590 Å and peak at 20440 Å . The emission component was also noted in SN 1994D and was attributed to Si III by Wheeler et al.

By maximum light the Mg II λ10926, Fe III, and Si II feature near 16500 Å became more prominent and a peak developed around 18100 Å. One week past maximum the spectrum was dramatically different and became dominated by strong absorption/emission features. The Mg II λ10926 line disappeared and a weak feature at 10000 Å became evident, possibly forming a P-Cygni profile. The most remarkable features were the strong and wide (FWHM $\sim$ 12,000 km s^{-1}) peaks attributed to blends of Co II, Fe II, and Ni II at 15500 and 17500 Å (Wheeler et al. 1998). Two weeks after maximum these peaks developed even further and new peaks appeared at 19900 and 21000 Å. A series of unidentified absorptions also could be observed in the J band at 10400, 10700, and 11100 Å. One month after maximum two additional broad emission peaks became evident at 22500 and 23600 Å which, according to Wheeler et al., are caused by iron-group elements (Co, Ni) as well as intermediate mass elements with appreciable contribution from Si. While the broad emissions appeared to redshift significantly as the SN evolved, the features that we identify as absorptions did not show any appreciable change in velocity.

3.2. SN 1999ex

Figure 4 displays the optical spectra of SN 1999ex in the SN rest-frame. The first spectrum, obtained on JD 2451496.62 (one day before B maximum), was characterized by a reddish continuum and several broad absorption/emission features due to Ca II H&K $\lambda\lambda$3934,3968, Fe II, Mg I, Na

I D $\lambda\lambda$5890,5896, Si II λ6355, and the Ca triplet with a clear P-Cygni profile. We also found convincing evidence for He I $\lambda\lambda$6678,7065 with expansion velocities of 6,000 km s^{-1} (similar to velocities displayed by the Fe, Mg, Na, Si, and O lines). It is possible that the feature at ∼4400 Å , usually attributed to a blend of Mg II and Fe II, had a contribution due to the He I λ4471. Likewise, the feature at ∼4800 Å could be a blend of Fe II λ4924 and He I λ4921, while the Na I D $\lambda\lambda$5890,5896 doublet could have a contribution from He I λ5876. Interstellar lines due to Na I D $\lambda\lambda$5890,5896, Ca II λ3934, and Ca II λ3968 were observed in absorption with equivalent widths of 2.8, 1.8, 0.9 Å, at the wavelengths corresponding to the rest-frame of the host galaxy. According to the correlation between equivalent widths and reddening for Galactic stars (Munari & Zwitter 1997), SN 1999ex was reddened by $E(B-V)$∼1.0±0.15. However, there appears to be a significant departure of SNe from this calibration (Hamuy et al. 2001), so this estimate is very uncertain.

The first spectrum of SN 1999ex bore quite resemblance to that of SN 1994I. Filippenko et al. (1995) argued that SN 1994I was a Type Ic event on the grounds that this object 1) did not show evidence for hydrogen lines (ruling out a Type II event), 2) had a Si II λ6355 line more subtle than in classical SNe Ia, and 3) He I λ5876 was absent or weak (and blended with Na D) (ruling out a Type Ib event). Based on the resemblance between these two spectra, we initially classified SN 1999ex as a Type Ic SN (Hamuy & Phillips 1999). However, the relatively stronger He lines displayed by SN 1999ex suggest that this object could well be an intermediate case between the Ib and Ic subclasses (we will return to this point in section 4.2). During the following two weeks the SN spectrum evolved slowly and most of the lines became stronger.

Figure 5 displays the IR spectra of SN 1999ex in the SN rest-frame. The most prominent feature in these spectra is the P-Cygni profile of He I λ10830 which was also observed in SN 1994I. The minimum of the absorption yields an expansion velocity of 8,000 km s^{-1}, in good agreement with the values derived from the optical spectra. The other evident feature is the P-Cygni profile due to He I λ20581, with the same expansion velocity. An unidentified absorption at 9970-10045 Å can be clearly seen, which should have a rest wavelength between 10200-10260 Å. A few weak unidentified lines can be seen also in the H band.

4. Discussion

4.1. SN 1999ee

Although Type Ia SNe display a large degree of spectroscopic homogeneity, there are several examples of SNe with spectral peculiarities. Different subclasses have been identified including SN 1991T-like objects, Branch-normal SNe, and SN 1991bg-like events (Branch et al. 1993). Recently, the Lick Observatory Supernova Survey (LOSS) produced a SN sample with well-understood selection effects (Li et al. 2001a) which permitted them to assess the intrinsic peculiarity rate of SNe Ia (Li et al. 2001b). This study showed that the sample of nearby SNe Ia comprises 20%, 64%, and 16% of 1991T-like, normal, and 1991bg-like objects, respectively.

Li et al. (2001a) defined a normal SN as one with prominent features due to Si II λ6355, Ca II H&K $\lambda\lambda$3934,3968, as well as additional lines of S II, O I, and Mg II around maximum light. The designation SN 1991T in such work is not strictly correct since the prototype of the 1991T class defined by Li et al. (2001b) is SN 1999aa. While SN 1999aa's main difference relative to normal SNe is just a relative weakness of the Si II λ6355 feature before maximum that becomes almost indistinguishable from normal SNe after peak (see Fig. 5 of Li et al. (2001b)), SN 1991T was a much more extreme event in the sense that the pre-maximum spectrum did not display the Ca II H&K $\lambda\lambda$3934,3968 blend shown by Branch-normal SNe, and also because it remained spectroscopically distinct several days after maximum (Phillips et al. 1992). For the sake of clarity, in what follows we refer to the 1991T-like events of Li et al. as 1999aa-like objects. The distinguishing feature of SN 1991bg-like objects is the Ti II absorption around 4100-4000 Å. There are many examples of intermediate class objects, which suggests a continuous spectral sequence among SNe Ia.

Because 1999aa-like events display slow-declining lightcurves (Δm$_{15}$(B)$\leq$1.0) and high peak luminosities, and 1991bg-like SNe show fast-decline rates (Δm$_{15}$(B)$\geq$1.7) and low peak luminosities, it is interesting to ask if the photometric behavior can be used to predict spectroscopic peculiarities. As a slow-declining (Δm$_{15}$(B)=0.94) and luminous (M_V=-19.94) event observed well before maximum light, SN 1999ee provides a good opportunity to investigate whether or not all luminous SNe display spectroscopic peculiarities before peak. To examine this point in detail Figure 6 (top) shows a comparison of the spectrum of SN 1999ee taken 9 days before B maximum to that of three other SNe including SN 1999aa with a decline rate of $\Delta m_{15}(B)$=0.75 (Krisciunas et al. 2000), the Calán/Tololo SN 1992bc with $\Delta m_{15}(B)$=0.87 (Hamuy et al. 1996), and the normal SN 1990N with $\Delta m_{15}(B)$=1.07 (Leibundgut et al. 1991; Lira et al. 1998). While SN 1999aa lacked the Si II λ6355 feature compared to the Branch-normal SN 1990N, both SN 1992bc and SN 1999ee displayed strong and well-defined Si features as early as ten days before peak. This shows that *not all slow-decliners are spectroscopically peculiar before maximum light.* As mentioned above, 1999aa-like events show a normal spectrum at peak brightness, which can be clearly appreciated in the bottom panel of Figure 6 from the spectra of SN 1999aa and SN 1999ee. The fact that the spectral differences displayed by the luminous SNe are only limited to the very first days of evolution suggests that the 1999aa-like and the Branch-normal SNe (represented here by SN 1999ee) are apparently similar explosions and that spectral diversity at early times probably reflects small differences in mixing or other chaotic behaviors rather than fundamental differences in the character of the explosions.

There are a handful of IR spectra published for SNe Ia (Meikle et al. 1996; Bowers et al. 1997; Hernández et al. 2000; Jha et al. 1999; Rudy et al. 2002). Höflich et al. (2002) recently observed SN 1999by and assembled the first continuous sequence of IR spectra for a SN Ia, extending from 3 days before maximum through day +15 after peak. To our knowledge the IR spectra of SN 1999ee – extending from day -9 to +42 – constitute the most complete IR spectroscopic sequence of a SN Ia and its Branch-normal nature makes it an ideal object in which to study the homogeneity of this class of objects at these wavelengths. We proceed now to address this issue from a sample of five SNe Ia encompassing a wide range in decline rates and optical spectroscopic properties. The

sample comprises the Branch-normal SN 1999ee, SN 1998bu (Jha et al. 1999; Hernández et al. 2000), and SN 1994D (Meikle et al. 1996), with $\Delta m_{15}(B)$=0.94,1.01,1.32, respectively (Phillips et al. 1999). [8] We also include SN 1999by ($\Delta m_{15}(B)$=1.90) which had optical spectra that showed resemblance to SN 1991bg (Garnavich et al. 2001), and SN 2000cx ($\Delta m_{15}(B)$=0.93) which shared some of the spectroscopic peculiarities displayed by SN 1999aa-like events (e.g. weak Si II λ6355) before maximum and a "sui generis" post-maximum behavior owing to unusually strong Fe III and weak Fe II lines (Li et al. 2001c).

Figure 7 (top) compares pre-maximum spectra of SN 2000cx, 1999ee, 1994D, and 1999by. The resemblance between the two Branch-normal SNe (1999ee and 1994D) is remarkable. The largest, yet subtle, difference was the Mg II λ10926 feature which was narrower and deeper in SN 1994D. The expansion velocities derived from the absorption minimum was quite similar, $\sim$10,500 km s^{-1}. Both the Si II and Si III features near 16500 Å and 20000 Å were clearly present on both SNe. With the exception of the high Mg II velocity ($\sim$20,000 km s^{-1}), SN 2000cx showed a normal featureless spectrum. Since magnesium is destroyed by oxygen burning, it is expected in material which experiences burning at the lowest densities near the surface. The high Mg velocity led Rudy et al. (2002) to conclude that nuclear burning in SN 2000cx extended farther out than in normal SNe, though it is equally likely that in this supernovae a blob containing carbon burning products drifted closer to the surface than in some other SNe Ia. The greater luminosity and slower decline of SN 2000cx argue for greater ^{56}Ni production, and this would manifest itself also in greater excitation in the ejecta. Indeed, SN 2000cx showed an emission feature at 12500 Å attributed to Fe III $\lambda\lambda$12786,12920,13003 (Rudy et al. 2002), which was also present in the normal SN 1999ee but at a lower strength, a weaker than normal Si II feature near 16500 Å, and a stronger Si III line around 20000 Å.

SN 1999by showed a pre-maximum spectrum noticeably different than that of normal SNe. The main difference was due to C I and O I lines, which were clearly absent in the spectra of other SNe. Höflich et al. (2002) suggested that nuclear burning in SN 1999by did not extend as far out as in normal SNe Ia. It is possible, however, that the presence of the C I and O I lines was due to a lower excitation evidenced by the smaller ^{56}Ni production, the low luminosity and fast decline of SN 1999by. The spectral differences are particularly evident in the J band. The Mg II λ10926 feature was deeper than normal, although its velocity of $\sim$10,000 km s^{-1} was similar to that observed in normal SNe. In the H band SN 1999by showed a strong broad emission feature due to a blend of Si II and Mg II lines which was also present in the other SNe but with a lower strength, presumably due to a weaker contribution from Mg II. The K band spectrum is also bumpier than normal due to Mg II lines.

Around maximum light the Mg II λ10926 feature was present in all three normal SNe (1999ee, 1998bu, and 1994D) with similar strengths and profiles (bottom panel of Figure 7). Meikle et al.

[8] We include in this comparison two spectra of SN 1998bu obtained by one of us (R.D.B.) with the CTIO 4-m Infrared Spectrograph on 1998 May 16 (3 days before B maximum) and June 3 (15 days after peak).

(1996) noted that the absorption minimum of the Mg II line did not show a shift in wavelength during the pre-maximum evolution of SN 1994D, as opposed to the optical lines which all redshifted with time as the photosphere receded through the ejecta. We confirmed the absence of any significant Doppler shift in Mg II from SN 1999ee which, according to Wheeler et al. (1998) was due to the fact that the photosphere had already receded below the inner edge of the magnesium layer at this early phase. It is interesting to note the absence in these spectra of the Ca II line near 11500 Å, a feature predicted by the models of Wheeler et al. (1998) that proves to be a useful diagnostic of the location of the transition layer between complete and incomplete silicon burning. The Si II absorption near 16500 Å and the spectral features in the K band were visible in the normal SNe 1999ee and 1998bu with a high degree of similarity. The pre-maximum spectral peculiarities of SN 1999by mentioned above were still evident near maximum light.

Figure 8 compares the post-maximum spectra available to us. Two weeks after peak the two normal SNe 1999ee and 1998bu displayed an impressive spectral homogeneity with strong peaks and valleys at 15000-17000 Å and 22000-26000 Å due to Fe II, Co II, Ni II, and Si II. The presence of Fe II, Co II, Ni II, and Si II is due to the ionization dropping predominantly to these ions, which happen to have strong lines in the near IR. The spectral differences of the fast-decliner SN 1999by persisted at this epoch. While its J spectrum had contributions from Ca II lines (Höflich et al. 2002) that were absent in SNe 1999ee and 1998bu, the broad emission around 15000-17000 Å was weaker than normal. At later epochs, the spectra of SNe 1999ee and 1998bu became much more complicated, yet their similarity remained remarkable.

As a result of this observational campaign we obtained the most complete optical/IR observations of a Type Ia SN, with an unprecedented wavelength and temporal coverage beginning nine days before maximum light. Moreover, since we were able to obtain the IR spectra within one or two days from the optical spectra, it was possible to combine these observations, as shown in Figure 9. This exercise revealed the excellent agreement between the optical and IR fluxes, a result that proved possible by synthesizing broad-band magnitudes and adjusting the flux scales according to the observed magnitudes. This optical/IR sequence shows that, while the pre-maximum optical spectrum was dominated by strong P-Cygni profiles of intermediate mass elements like Ca II, Si II, Mg II, S II, the IR was characterized by a smooth, almost featureless continuum. By maximum light, on the other hand, the IR spectrum was already dominated by broad features, and one week later the IR flux was mostly powered by emission lines of iron group elements like Co II, Fe II, and Ni II (freshly synthesized in the innermost layers of the ejecta) that were particularly prominent in the H and K bands. At the same time a dramatic flux dip around 12000 Å began to develop. Previous spectroscopic observations have already revealed this J-band deficit in other SNe Ia (Bowers et al. 1997), which is responsible for the red $J - H$ color displayed by SNe Ia after maximum light (Elias et al. 1985).

This spectral sequence lends support to the suggestion by Spyromilio, Pinto, & Eastman (1994) and Pinto & Eastman (2000) that the "photosphere" recedes rapidly to the center of the supernova in the IR while at optical wavelengths the greater opacity arising from the higher spectral density

of lines keeps the photosphere at higher velocities. Emission at longer wavelengths increases after maximum light due to a shift in ionization to more-neutral species which have greater emissivity in the near IR. In this model, the J-band deficit is due to the relative absence of lines (and hence opacity) in the 12000 Å region rather than increasing opacity. Likewise, the secondary maxima exhibited by the JHK lightcurves ∼30 days after B maximum (Elias et al. 1981, 1985; Jha et al. 1999; Hernández et al. 2000; Krisciunas et al. 2000) are due to the increasing release of energy through lower-optical depth IR transitions. The prominent post-maximum emission features displayed by SN 1999ee in the H and K bands lend support to this picture.

4.2. SN 1999ex

SNe are classified according to their spectral features near maximum light (Filippenko 1997). Type II SNe are characterized by prominent hydrogen features and are believed to arise from the core collapse of massive ($>$ 8-10 $M_\odot$) stars. The common feature in all Type I SNe is the lack of hydrogen spectral lines. The strong Si II λ6355 is the defining feature of SNe Ia. Their occurrence in all type of stellar environments has led to the general consensus that the progenitors of SNe Ia are white dwarfs that undergo thermonuclear disruption after a period of mass transfer from binary companions. The proximity of SNe Ib and Ic to massive star formation regions (Van Dyk et al. 1996), on the other hand, provides evidence that these objects result from the core collapse of massive stars. The lack of hydrogen in their spectra is attributed to the loss of their outer hydrogen envelopes by stellar winds or mass transfer to binary companions. There is growing evidence for a close physical connection between SNe II and SNe Ib from the observations of SNe 1987K, 1993J, and 1996cb, which evolved from SNe II at early epochs to SNe Ib at later times (Filippenko 1988; Filippenko et al. 1993; Qiu et al. 1999). The distinguishing difference between Type Ib and Ic SNe are the *optical* He I lines, which are conspicuous in SNe Ib and weak or absent in SNe Ic. It is still a matter of debate whether SNe Ic constitute an extreme case of SNe Ib or a completely separate class of objects. The apparent absence of He in the spectra of SNe Ic motivated the idea that the progenitors of these objects could be nearly bare C+O cores of massive stars (Wheeler & Harkness 1990) that loose most of their helium by binary transfer or strong stellar winds. However, Woosley et al. (1995) showed that helium stars could be the progenitors of both SNe Ib and SNe Ic. They showed that the presence or absence of He I lines in the spectrum is determined primarily by the amount of mixing, not the amount of helium present – greater mixing of radioactive material increases the excitation of helium leading to stronger lines.

Significant effort has been put over recent years into determining the presence of helium in the spectra of SNe Ic in order to better understand the nature of these objects. A detailed inspection of the spectra of the Type Ic SN 1994I led Filippenko et al. (1995) to conclude that weak He I lines were probably present in the optical region and that He I λ10830 was very prominent, although its Doppler shift implied an unusually high expansion velocity ∼16,600 km s^{-1}. Clocchiatti et al. (1996) confirmed these observations and found evidence that He I λ5876 was also present in

SN 1994I with a blueshift of ∼17,800 km s^{-1}. They also reported high velocity He I λ5876 in the spectra of the three best-observed Type Ic SNe (1983V, 1987M, and 1988L), which led them to conclude that most, and probably all, SNe Ic show evidence for optical He I lines. This conclusion, however, was recently questioned by Millard et al. (1999) and Baron et al. (1999) by means of spectral synthesis models which showed that the IR feature near 10250 Å could be accounted with lines of C I and Si I. Moreover, Baron et al. (1999) argued that the feature attributed to He I λ5876 in the spectrum of SN 1994I could be a blend of other species. Evidently, there is no consensus yet about the presence or absence of He in the spectra of SNe Ic.

Recently Matheson et al. (2001) compiled and analyzed a large collection of spectra of SNe Ib and Ic. This study showed no compelling evidence for He in the spectra of SNe Ic and no gradual transition from the Ib to the Ic class, which supported the idea that these objects are produced by different progenitors.

Our optical spectra of SN 1999ex show evidence for He I absorptions of moderate strength in the optical region, thus suggesting the existence of an intermediate Ib/c case. To illustrate this point in Figures 10 and 11 we show a comparison between SN 1999ex, the best-observed Type Ic SN 1994I, and the prototypes of the Ib (SN 1984L) and Ic class (SN 1987M). The near-maximum spectra (top panel of Figure 10) reveal a gradual increase in the strength of all He lines (indicated with tick marks) from the Ic to the Ib class. In the bottom panel of Figure 10 (one week past maximum) it is possible to see that, even though the spectra of the Type Ic SNe 1994I and 1987M are quite similar, SN 1994I shows deeper troughs at the wavelengths of the He I lines, especially at 4471, 4921, and 5876 Å. The spectrum of SN 1994I obtained two weeks past maximum (Figure 11) is particularly interesting as it provides good evidence that the He I λ5876 line was indeed present in the spectrum of SN 1994I with a higher expansion velocity than the Na I D λ5893 doublet. This was also noted by Filippenko et al. (1995) who quoted an expansion velocity of ∼16,600 km s^{-1} for the He line (see also Clocchiatti et al. (1996) for a detailed discussion). Overall, Figures 10-11 reveal that there is a smooth spectroscopic sequence ranging from the He deficient Type Ic SNe 1987M and 1994I, the Type Ib/c SN 1999ex, and the Type Ib SN 1984L that is characterized by strong optical He lines. We conclude therefore that SN 1999ex provides first evidence for a link between the Ib and Ic classes and that there is a continuous sequence of SNe Ib and Ic objects.

Special attention must be paid to the IR feature near 11,000 Å which was very prominent in SNe 1999ex and 1994I. As mentioned above the definitive identity of this feature in SN 1994I is still uncertain: it could be accounted with lines of C I and Si I (Millard et al. 1999; Baron et al. 1999) or with high velocity He I λ10830 (Filippenko et al. 1995; Clocchiatti et al. 1996). If the feature in SN 1999ex was He I λ10830 it would imply a moderate velocity of 6,000-8,000 km s^{-1}, which matches very well the velocities derived from the Fe, Na and Si lines. The presence of the He I λ20581 with the same expansion velocity (see Figure 5) suggests that the IR feature in SN 1999ex was indeed due to He I λ10830. Altogether our IR spectra of SN 1999ex provide unambiguous proof that He was present in the atmosphere of this intermediate Ib/c object. A detailed atmosphere model could be very useful at placing limits on the He mass in the ejecta of

SN 1999ex and constraining the nature of its progenitor. As suggested by Clocchiatti et al. (1996) the presence of highly blueshifted He I λ5876 in SN 1994I suggests that the IR feature was also due to He I λ10830. If so, the difference in He velocities between SNe 1994I and 1999ex might prove an interesting clue to the underlying physics of the atmospheres of this class of objects. Further optical/IR spectroscopy and photometry will lead us to better understanding the atmospheres of SNe Ib and Ic.

Finally, given that the IR spectra were obtained within one day from the optical spectra, we were able to combine these observations. Figure 12 shows the resulting spectra and the excellent agreement between the optical and IR fluxes. Note the prominent He I $\lambda\lambda$10830,20581 features.

4.3. Maximum-light optical/IR spectra of SNe

In the course of the SOIRS program we obtained high-quality spectroscopy of the Type II SN 1999em (Hamuy et al. 2001). Figure 13 compares maximum-light spectra of the Type II SN 1999em, the Type Ib/c SN 1999ex, and the Type Ia SN 1999ee. This figure permits one to compare the different characters of the main classes of SNe, all the way from 3,000 to 25,000 Å. The Type II is distinguished by prominent hydrogen Balmer and Paschen lines. It also shows the P-Cygni profile of the He I λ10830 transition. The Type Ib/c is characterized by the strong He I $\lambda\lambda$10830,20581 lines in the IR, the He I λ5876 line in the optical, and other lines in the optical due to singly ionized Ca, Fe, Mg, Si and neutral Na and O. It is interesting to note that, while both the Type II and the Type Ib/c show strong He I λ10830, only the Type Ib/c shows a significant He I λ20581 feature. Finally, the Type Ia at the bottom of this figure is characterized by the strong Si II λ6355 and other intermediate-mass elements, and the absence of hydrogen and helium.

5. Conclusions

The observations obtained for SN 1999ee constitute the most complete spectral and temporal coverage ever achieved for a SN Ia. Its Branch-normal character makes it an ideal reference for comparative studies of SNe Ia.

Before maximum light SN 1999ee displayed a normal spectrum with a strong Si II λ6355 absorption, thus showing that not all slow-declining SNe are spectroscopically peculiar at these evolutionary phases. We conclude that the photometric properties of luminous SNe Ia cannot be used to predict spectroscopic peculiarities.

From a comparison of the IR spectra of SN 1999ee and other SNe Ia that encompass a wide range in decline rates we find that there is a remarkable homogeneity among the Branch-normal SNe Ia during their first 60 days of evolution. Although the slow-decliner luminous SN 2000cx showed a premaximum featureless IR spectrum similar to that of normal SNe, the Mg II λ10926

line was characterized by a high expansion velocity. The fast-decliner subluminous SN 1999by was noticeably different than the other SNe at all epochs. This study reveals that the spectroscopic peculiarities displayed by SN 1991bg-like objects at optical wavelengths are also present in the IR.

The fortunate occurrence of SN 1999ex within three weeks and in the same galaxy that hosted SN 1999ee permitted us to obtain optical and IR spectroscopy of a Ib/c event. SN 1999ex was characterized for the lack of hydrogen lines, weak optical He I lines, and strong He I λ10830,20581, thus providing an example of an intermediate case between pure Ib and Ic SNe. We conclude therefore that SN 1999ex provides first clear evidence for a link between the Ib and Ic classes and that there is a continuous spectroscopic sequence ranging from the He deficient SNe Ic to the SNe Ib which are characterized by strong optical He I lines.

M. H. is very grateful to Las Campanas and Cerro Calán observatories for allocating an office and providing generous operational support to the SOIRS program during 1999-2000. M. H. and J. M. thank the ESO, CTIO, and Las Campanas visitor support staffs for their assistance in the course of our observing runs, and the Director General of ESO for allocating Director's discretionary telescope time to this project. We are very grateful to A. Filippenko, P. Höflich, S. Jha, D. Leonard, W. Li, P. Meikle, R. Rudy, and J. Spyromilio, for making us available their spectra of SNe 1984L, 1987M, 1994D, 1994I, 1999by, 1998bu, and 2000cx. Support for this work was provided by NASA through Hubble Fellowship grant HST-HF-01139.01-A awarded by the Space Telescope Science Institute, which is operated by the Association of Universities for Research in Astronomy, Inc., for NASA, under contract NAS 5-26555. J.M. acknowledges support from FONDECYT grant 1980172. This research has made use of the NASA/IPAC Extragalactic Database (NED), which is operated by the Jet Propulsion Laboratory, California Institute of Technology, under contract with the National Aeronautics and Space Administration. This research has made use of the SIMBAD database, operated at CDS, Strasbourg, France.

REFERENCES

Axelrod, T. S. 1980, Ph. D. thesis, Univ. California at Santa Cruz

Baron, E., Branch, D., Hauschildt, P. H., Filippenko, A. V., & Kirshner, R. P. 1999, ApJ, 527, 739

Bowers, E. J. C., Meikle, W. P. S., Geballe, T. R., Walton, N. A., Pinto, P. A., Dhillon, V. S., Howell, S. B., & Harrop-Allin, M. K. 1997, MNRAS, 290, 663

Branch, D., Fisher, A., & Nugent, P. 1993, AJ, 106, 2383

Clocchiatti, A., Wheeler, J. C., Brotherton, M. S., Cochran, A. L., Wills, D., Barker, E. S., & Turatto, M. 1996, ApJ, 462, 462

Elias, J. H, Frogel, J. A., Hackwell, J. A., & Persson, S. E. 1981, ApJ, 251, L13

Elias, J. H, Matthews, K., Neugebauer, G., & Persson, S. E. 1985, ApJ, 296, 379

Filippenko, A. V. 1988, AJ, 96, 1941

Filippenko, A. V., Matheson, T., & Ho, L. C. 1993, ApJ, 415, L103

Filippenko, A. V., et al. 1995, ApJ, 450, L11

Filippenko, A. V. 1997, ARA&A, 35, 309

Garnavich, P. M., et al. 2001, ApJ, submitted (astro-ph/0105490)

Gray, R. O., & Corbally, C. J. 1994, AJ, 107, 742

Hamuy, M., Suntzeff, N. B., Heathcote, S. R., Walker, A. R., Gigoux, P., & Phillips, M. M. 1994, PASP, 106, 566

Hamuy, M., et al. 1996, AJ, 112, 2408

Hamuy, M., & Phillips, M. M. 1999, IAUC 7310

Hamuy, M., et al. 2001, ApJ, 558, 615

Hernández, M., et al. 2000, MNRAS, 319, 223

Höflich, P., Khokhlov, A. M., & Wheeler, J. C. 1995, ApJ, 444, 831

Höflich, P., Gerardy, C. L., Fesen, R. A., & Sakai, S. 2002, ApJ, in press (astro-ph/0112126)

Jha, S., et al. 1999, ApJS, 125, 73

Krisciunas, K., Hastings, N. C., Loomis, K., McMillan, R., Rest, A., Riess, A. G., & Stubbs, C. 2000, ApJ, 539, 658

Krisciunas, K., et al. 2002, in preparation

Leibundgut, B., Kirshner, R. P., Filippenko, A. V., Shields, J., C., Foltz, C. B., Phillips, M. M., & Sonneborn, G. 1991, ApJ, 371, L23

Li, W., Filippenko, A. V., & Riess, A. G. 2001a, ApJ, 546, 719

Li, W., Filippenko, A. V., Treffers, R. R., Riess, A. G., Hu, J., & Qiu, Y. L. 2001b, ApJ, 546, 734

Li, W., et al. 2001c, PASP, 113, 1178

Lira, P., et al. 1998, AJ, 115, 234

Maiolino, R., Rieke, G. H., & Rieke, M. J. 1996, AJ, 111, 537

Matheson, T., Filippenko, A. V., Li, W., Leonard, D. C., & Schields, J. C. 2001, AJ, 121, 1648

Maza, J., & Hamuy, M., IAUC 7272

Meikle, W. P. S, et al. 1996, MNRAS, 281, 263

Millard, J., et al. 1999, ApJ, 527, 746

Moorwood, A. F. 1997, in Proc. SPIE, Vol. 2871, 1146

Munari, U., & Zwitter, T. 1997, A&A, 318, 269

Phillips, M. M, Wells, L. A., Suntzeff, N. B., Hamuy, M., Leibundgut, B., Kirshner, R. P., & Foltz, C. B. 1992, AJ, 103, 1632

Phillips, M. M, Lira, P., Suntzeff, N. B., Schommer, R. A., Hamuy, M., & Maza, J. 1999, AJ, 118, 1766

Pinto, P. A., & Eastman, R. G. 2000, ApJ, 530, 757

Qiu, Y., Li. W., Qiao, Q., & Hu, J. 1999, AJ, 117, 736

Rudy, R. J., Lynch, D. K., Mazuk, S., Venturini, C. C., Puetter, R. C., & Höflich, P. 2002, ApJ, 565, 413

Schlegel, D. J., Finkbeiner, D. P., & Davis, M. 1998, ApJ, 500, 525

Spyromilio, J., Pinto, P. A., & Eastman, R. G. 1994, MNRAS, 266, L17

Stritzinger, M., et al. 2002, in preparation

Van Dyk, S. D., Hamuy, M., & Filippenko, A. V. 1996, AJ, 111, 2017

Wheeler, J. C., & Harkness, R. P. 1990, Rep. Prog. Phys., 53, 1467

Wheeler, J. C., Höflich, P., Harkness, R. P., & Spyromilio, J. 1998, ApJ, 496, 908

Woosley, S. E., Langer, N., & Weaver, T. A. 1995, ApJ, 448, 315

Table 1. Journal of the Spectroscopic Observations

UT Date	Julian Date -2451000	Observ-atory	Telescope	Instr-ument	Detector	Grating/ Grism	Order	Wavelength (μm)	Dispersion (Å/pix)	Weather	Observer(s)
1999 Oct 09	460.53	Paranal	VLT/Antu	ISAAC	Rockwell1K	···	5,4,3,2	0.98-2.50	2.9,3.6,4.7,7.1	Clear	Hamuy,Lidman
1999 Oct 09	460.56	Tololo	4-m	R-C Spec.	Loral3Kx1K	KPGL-2	1	0.33-0.87	1.9	Cirrus	Maza
1999 Oct 11	462.52	La Silla	NTT	EMMI	TEK1024+2048	5,13	1	0.33-1.01	2.7,3.5	Clear	Hamuy,Doublier
1999 Oct 16	467.56	Campanas	2.5-m	WFCCD	TEK2048	Blue	···	0.36-0.92	3.0	Clouds?	Phillips
1999 Oct 18	469.49	La Silla	NTT	SOFI	Rockwell1K	Red	···	1.50-2.53	10.2	Clear	Doublier,Maza
1999 Oct 18	469.60	La Silla	NTT	EMMI	TEK1024+2048	5,13	1	0.33-1.00	2.7,3.5	Clear	Maza
1999 Oct 19	470.50	Paranal	VLT/Antu	ISAAC	Rockwell1K	···	5,4,3,2	0.98-2.50	2.9,3.6,4.7,7.1	Clear	Hamuy,Cuby,Petr
1999 Oct 20	471.56	La Silla	D1.5-m	DFOSC	Loral2Kx2K	3,5	1	0.33-0.98	2.3,3.1	···	Pompei
1999 Oct 22	473.61	La Silla	NTT	SOFI	Rockwell1K	Blue,Red	···	0.95-2.47	7.0,10.2	Clear	Hainaut,Lefloc'h
1999 Oct 25	476.51	La Silla	D1.5-m	DFOSC	Loral2Kx2K	3,5	1	0.33-0.98	2.3,3.1	Clear	Augusteyn
1999 Oct 26	477.48	La Silla	NTT	SOFI	Rockwell1K	Blue,Red	···	0.95-2.46	7.0,10.2	···	Hainaut,Vanzi
1999 Oct 27	478.52	Tololo	1.5-m	R-C Spec.	Loral1.2Kx0.8K	58	2	0.37-0.50	1.1	Clear	Olsen
1999 Oct 29	480.51	La Silla	D1.5-m	DFOSC	Loral2Kx2K	3,5	1	0.34-0.98	2.3,3.1	···	Augusteyn
1999 Nov 02	484.49	Paranal	VLT/Antu	ISAAC	Rockwell1K	···	5,4,3,2	0.98-2.50	2.9,3.6,4.7,7.1	Clear	Hamuy,Lidman,Petr
1999 Nov 03	485.62	La Silla	NTT	EMMI	TEK1024+2048	5,13	1	0.33-1.01	2.7,3.5	···	Maza
1999 Nov 06	488.52	La Silla	NTT	SOFI	Rockwell1K	Blue	···	0.94-1.65	7.0	Clear	Brillant
1999 Nov 06	488.53	La Silla	D1.5-m	DFOSC	Loral2Kx2K	3,5	1	0.34-0.98	2.3,3.1	Clear?	Augusteyn
1999 Nov 09	491.50	La Silla	NTT	SOFI	Rockwell1K	Blue,Red	···	0.95-2.51	7.0,10.2	Clear	Hamuy,Brillant
1999 Nov 09	491.62	La Silla	NTT	EMMI	TEK1024+2048	5,13	1	0.34-1.00	2.7,3.5	Clear	Hamuy,Brillant
1999 Nov 14	496.56	La Silla	NTT	SOFI	Rockwell1K	Blue,Red	···	0.95-2.46	7.0,10.2	Clear	Hamuy,Doublier
1999 Nov 14	496.62	La Silla	NTT	EMMI	TEK1024+2048	5,13	1	0.34-1.00	2.7,3.5	Clear	Hamuy,Doublier
1999 Nov 18	500.53	Paranal	VLT/Antu	ISAAC	Rockwell1K	···	5,4,3,2	0.98-2.50	2.9,3.6,4.7,7.1	Clear	Serv. Obs.
1999 Nov 19	501.58	La Silla	NTT	EMMI	TEK1024+2048	5,13	1	0.34-1.00	2.7,3.5	Clear	Hamuy,Doublier
1999 Nov 28	510.52	Paranal	VLT/Antu	ISAAC	Rockwell1K	···	5,4,3,2	0.98-2.50	2.9,3.6,4.7,7.1	Clear	Hamuy,Lidman,Chadid
1999 Nov 28	510.63	La Silla	D1.5-m	DFOSC	Loral2Kx2K	3,5	1	0.40-0.98	2.3,3.1	···	Pinfield

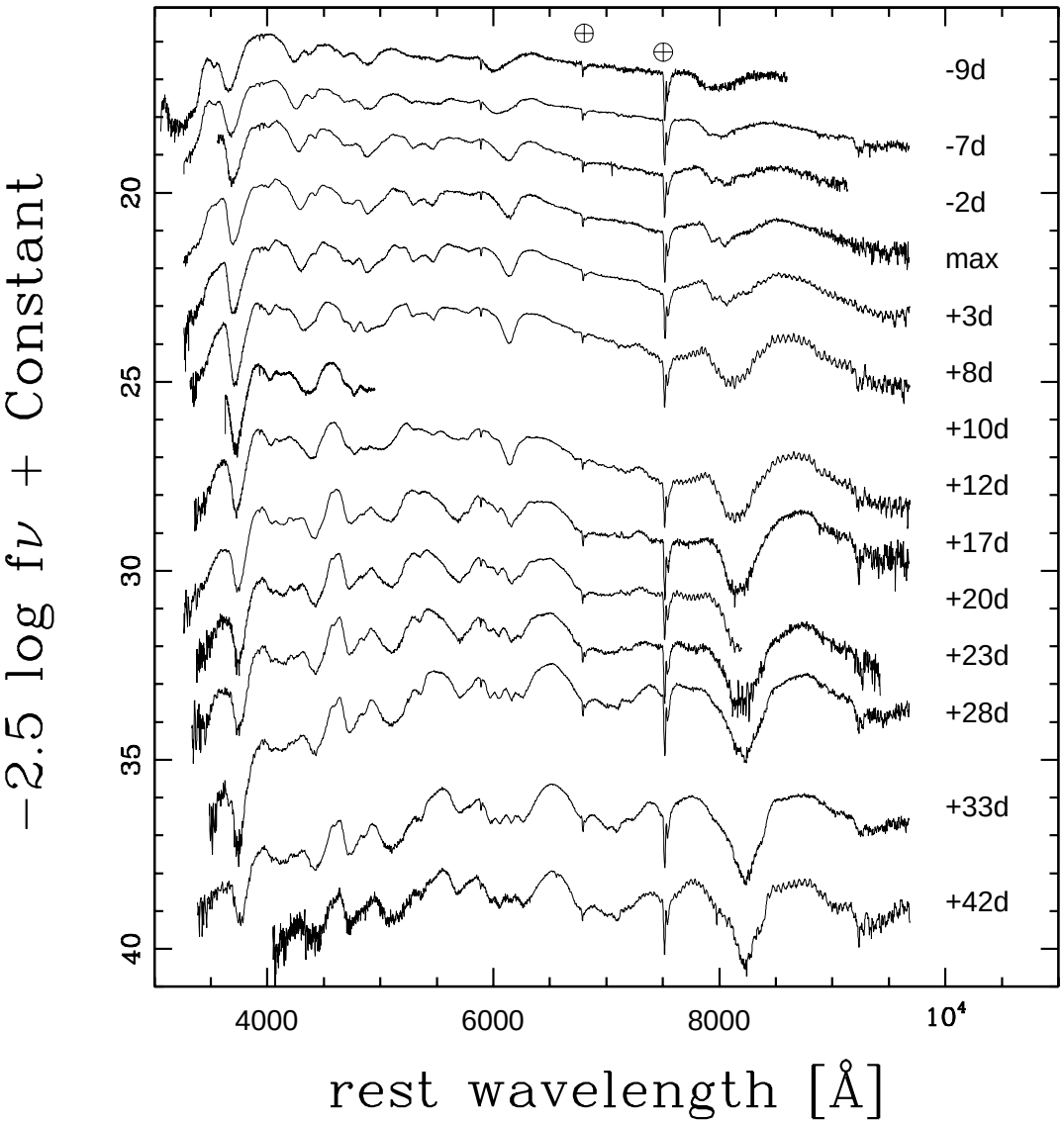

Fig. 1.— Optical spectroscopic evolution of SN 1999ee in AB magnitudes. Time (in days) since B maximum is indicated for each spectrum. The $\oplus$ symbols show the main telluric features.

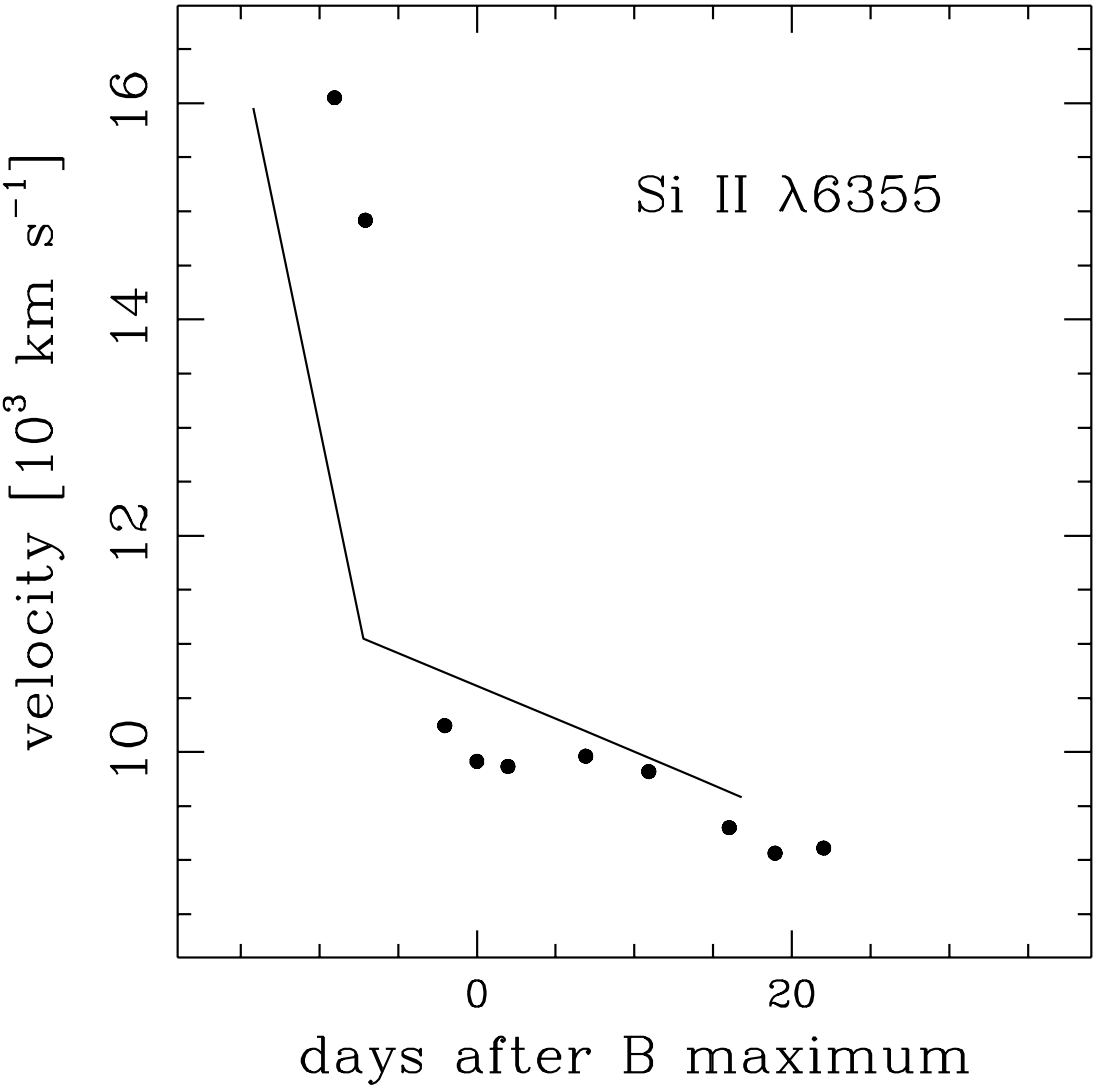

Fig. 2.— Expansion velocities derived from the absorption minima of Si II λ6355 for SN 1999ee, after correcting for the recession velocity of the host galaxy. The solid line corresponds to SN 1990N.

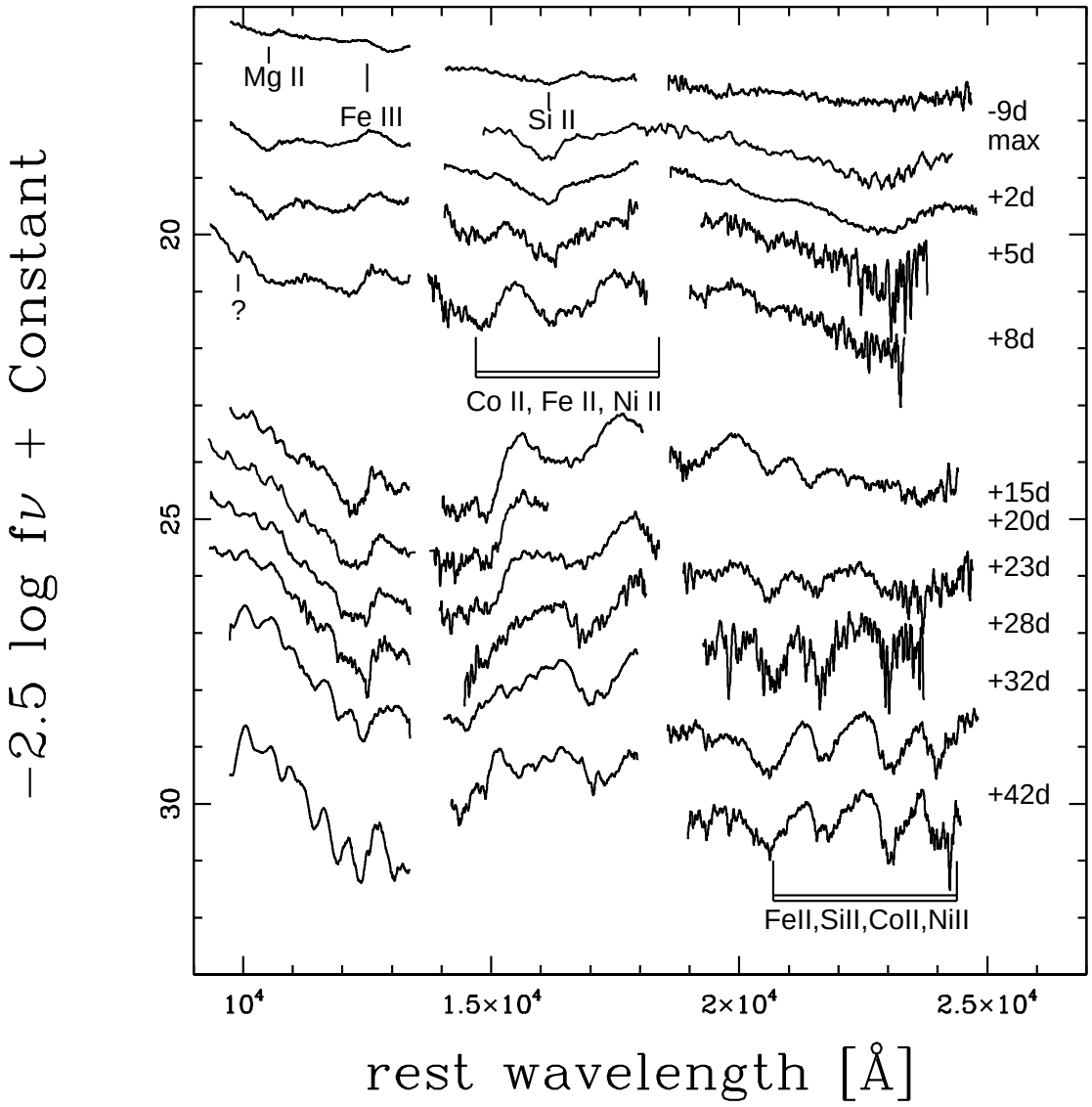

Fig. 3.— IR spectroscopic evolution of SN 1999ee in AB magnitudes. The most prominent features are labeled. Time (in days) since B maximum is indicated for each spectrum.

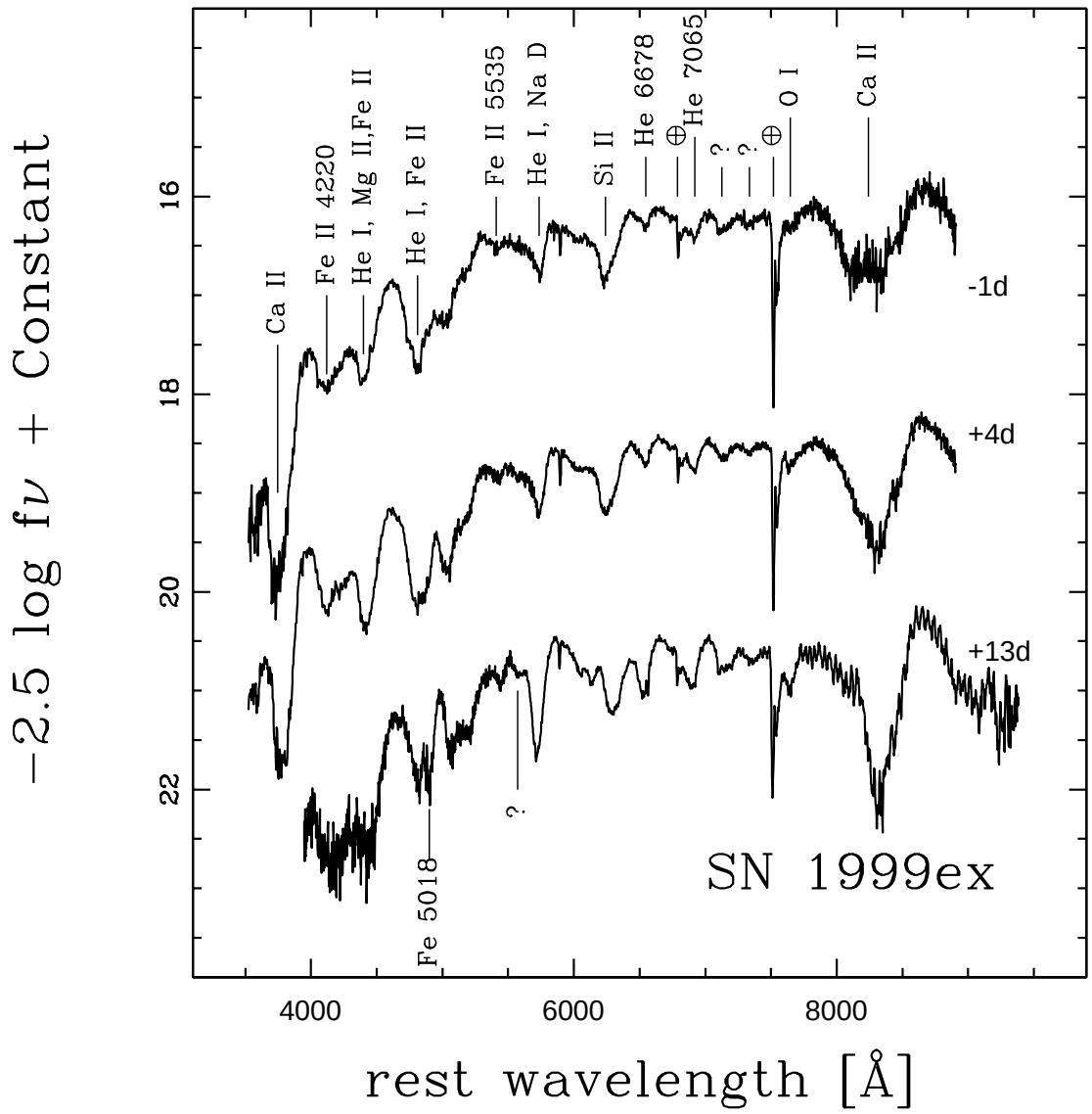

Fig. 4.— Optical spectroscopic evolution of SN 1999ex in AB magnitudes. Time (in days) since B maximum is indicated for each spectrum. The most prominent features are labeled as well as the main telluric features with the $\oplus$ symbol.

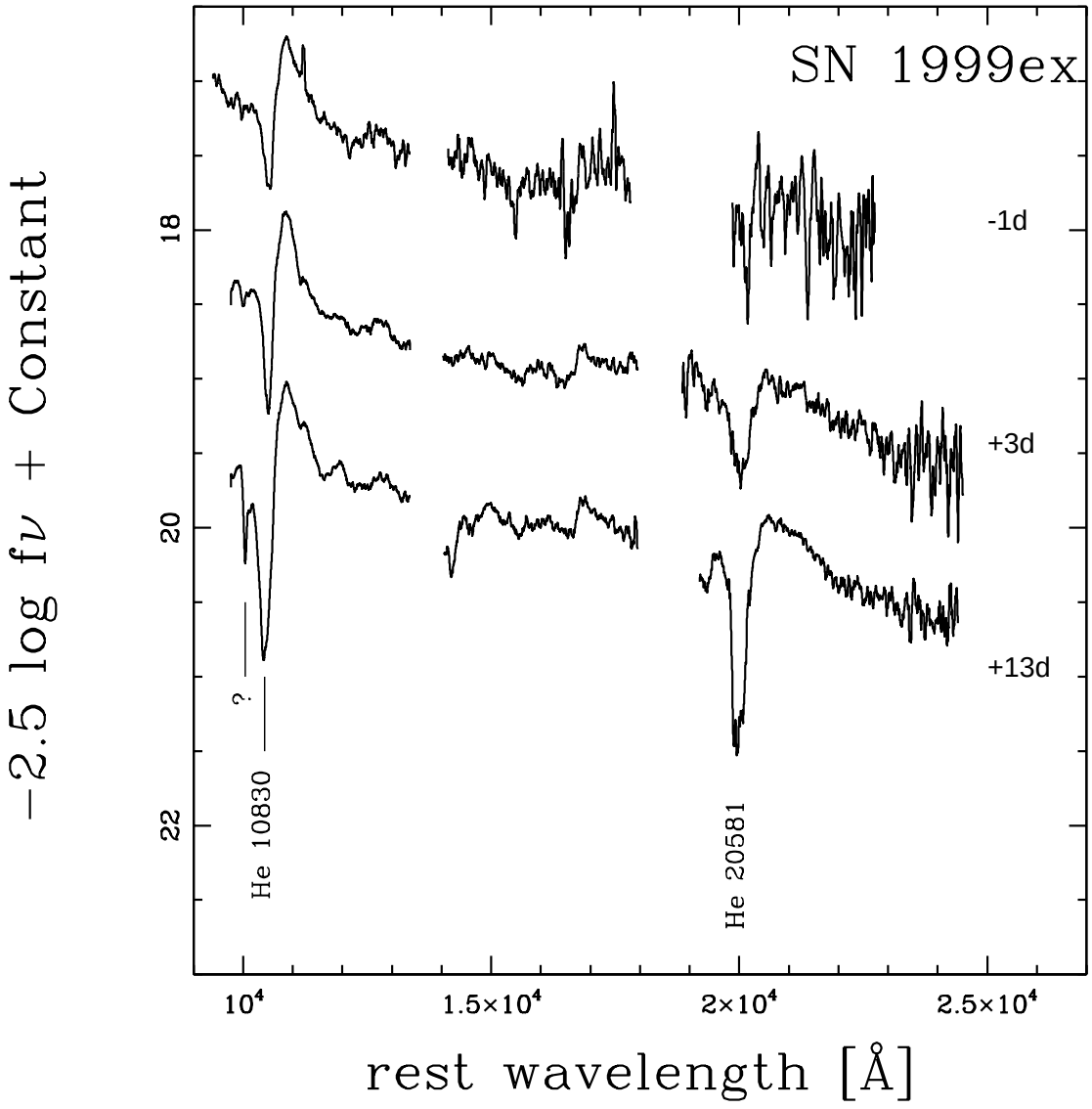

Fig. 5.— IR spectroscopic evolution of SN 1999ex in AB magnitudes. The two most prominent features are due to He I, while the absorption at 10,000 Å remains unidentified. Time (in days) since B maximum is indicated for each spectrum.

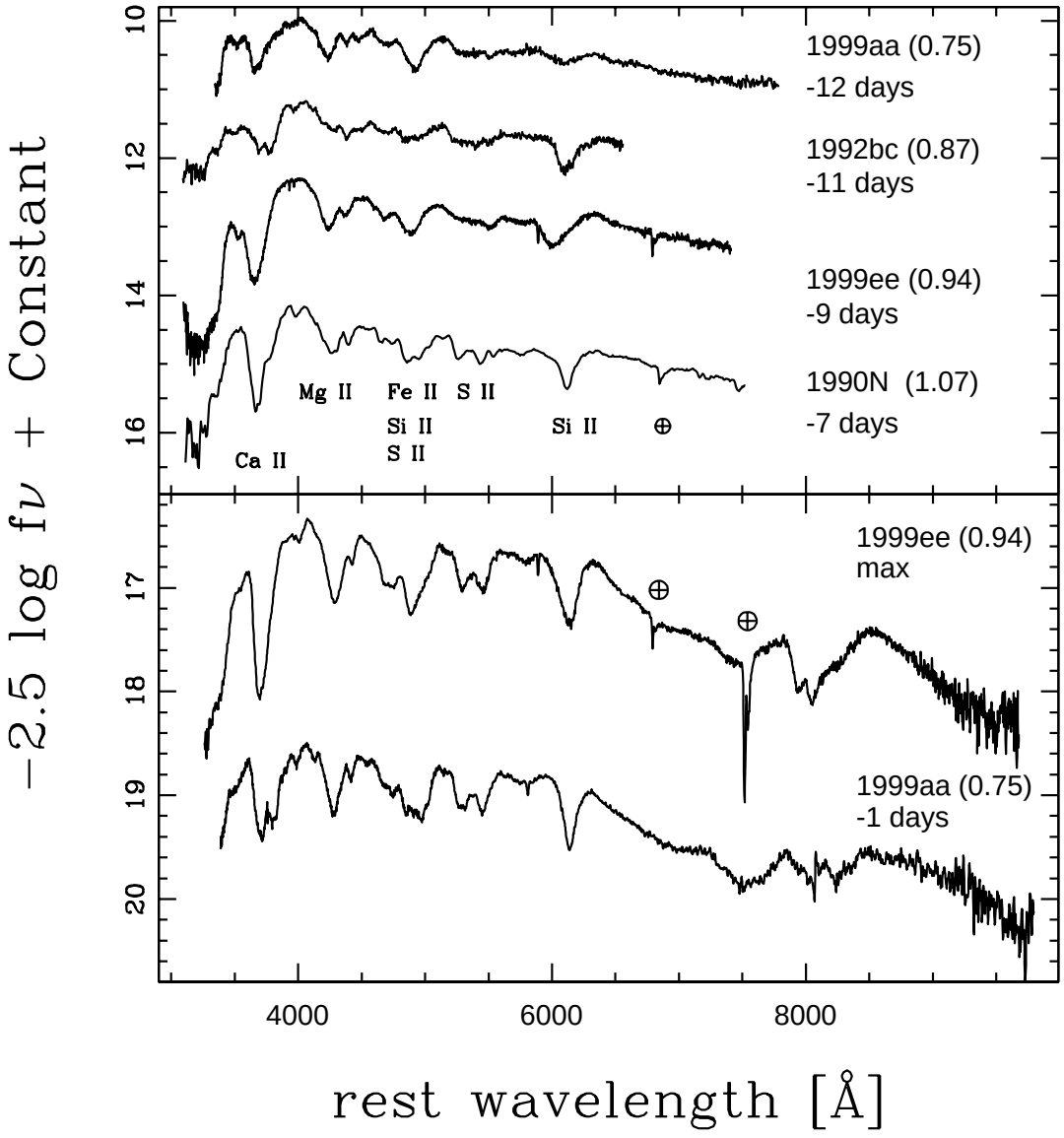

Fig. 6.— (top) Comparison of the optical spectra of three slow-declining SNe Ia and the Branch-normal SN 1990N obtained about 10 days before B maximum (top). The spectra have been shifted with respect to each other by arbitrary amounts to facilitate the comparison. In parenthesis are given the decline rates $\Delta m_{15}(B)$ for each SN. (bottom) Same as above but for SN 1999aa and SN 1999ee near maximum light.

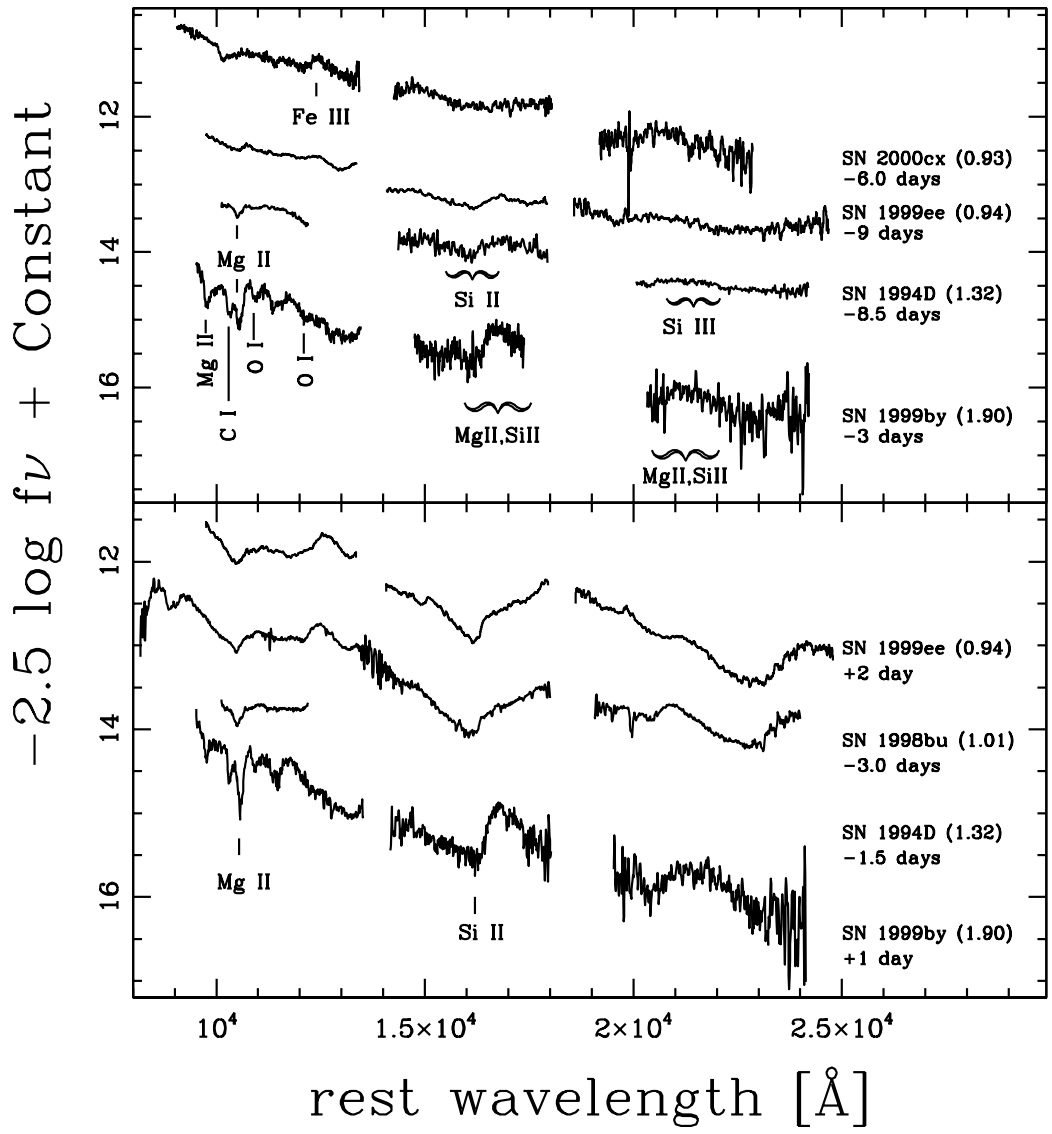

Fig. 7.— Comparison of the pre-maximum and maximum-light IR spectra of SNe 1994D, 1998bu, 1999by, 1999ee, and 2000cx. Time (in days) since B maximum is indicated for each spectrum along with the decline rates $\Delta m_{15}(B)$.

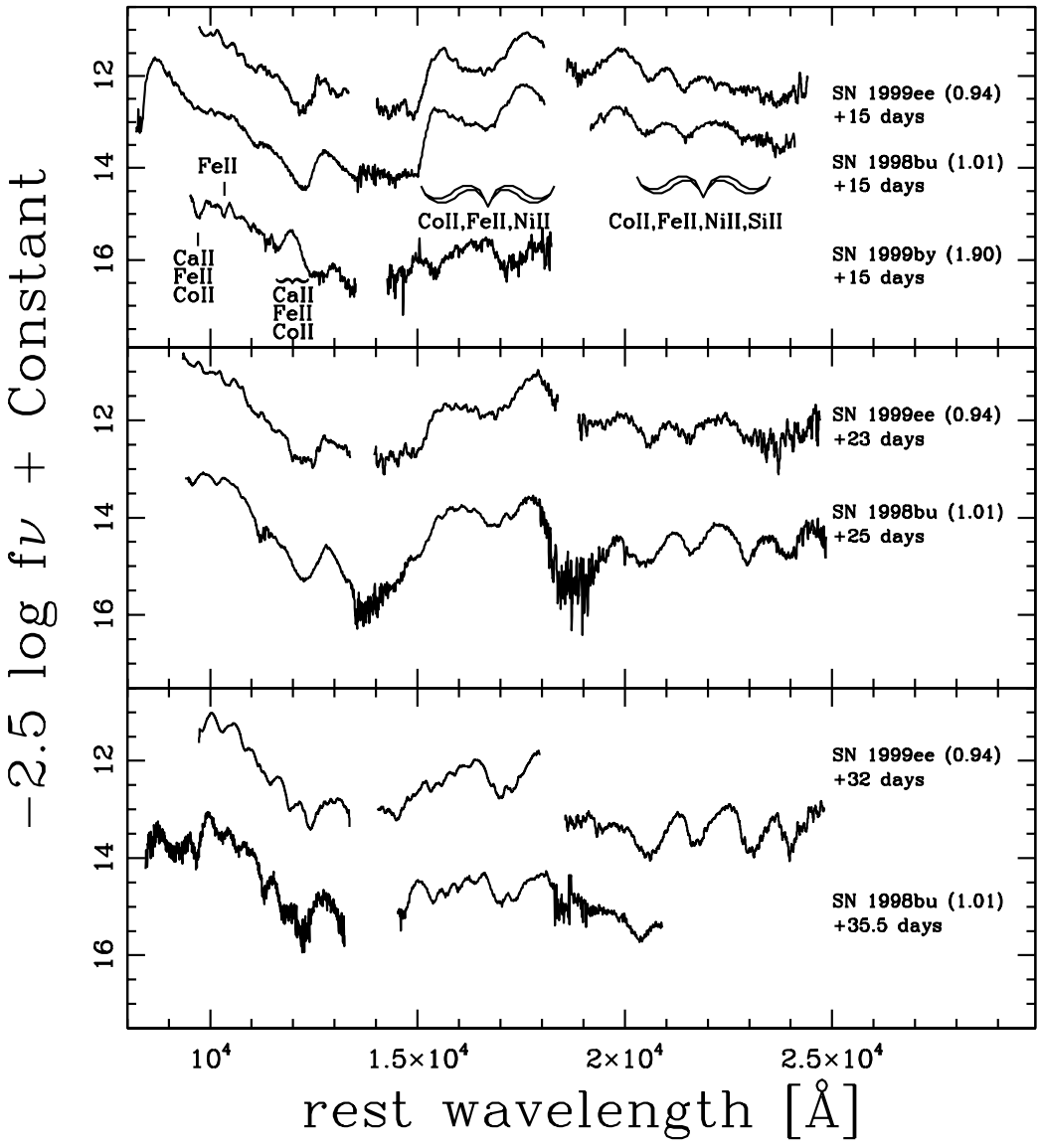

Fig. 8.— Comparison of the post-maximum IR spectra of SNe 1998bu, 1999by, and 1999ee. Time (in days) since B maximum is indicated for each spectrum along with the decline rates $\Delta m_{15}(B)$.

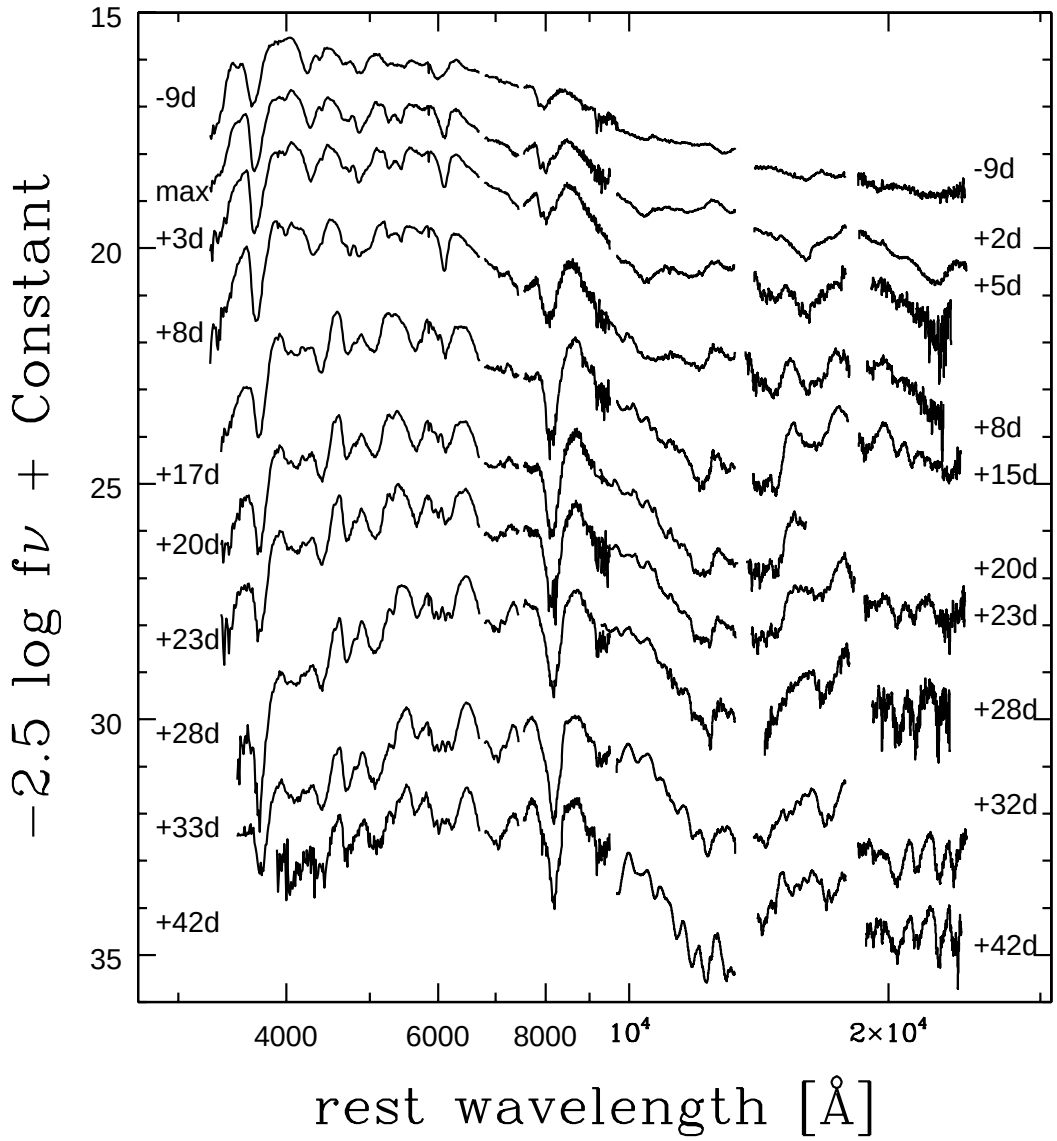

Fig. 9.— Combined optical and IR spectra of SN 1999ee in AB magnitudes. Time (in days) since B maximum is indicated for each spectrum.

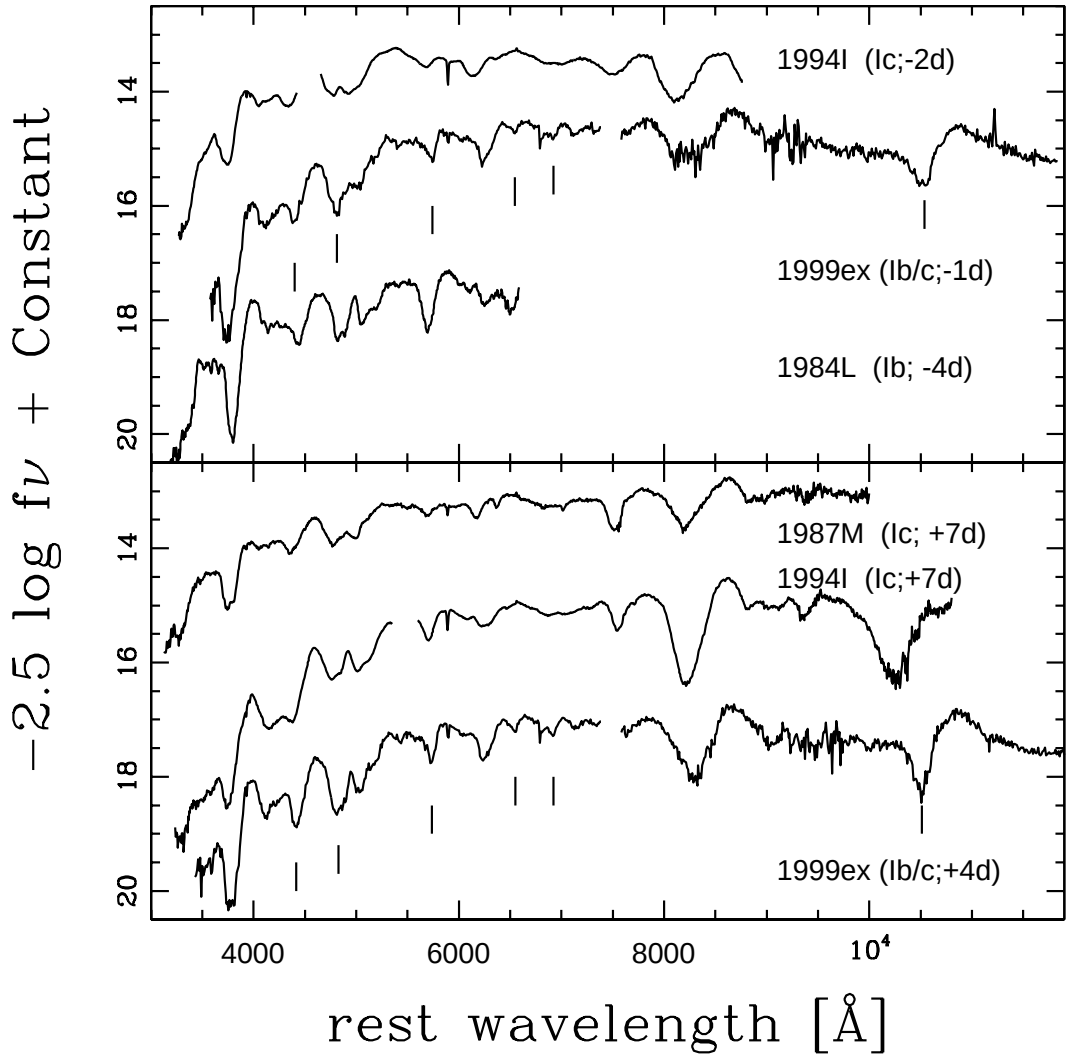

Fig. 10.— Comparison of near-maximum spectra of the Type Ib/c SN 1999ex with the prototype of the Ib class SN 1984L, and the Type Ic SNe 1994I and 1987M. Tick marks indicate the He I lines in the SN 1999ex spectra. The strengths of the He lines gradually increase from the Type Ic to the Ib SN, and SNe 1999ex appears to bridge the separation between these two subclasses.

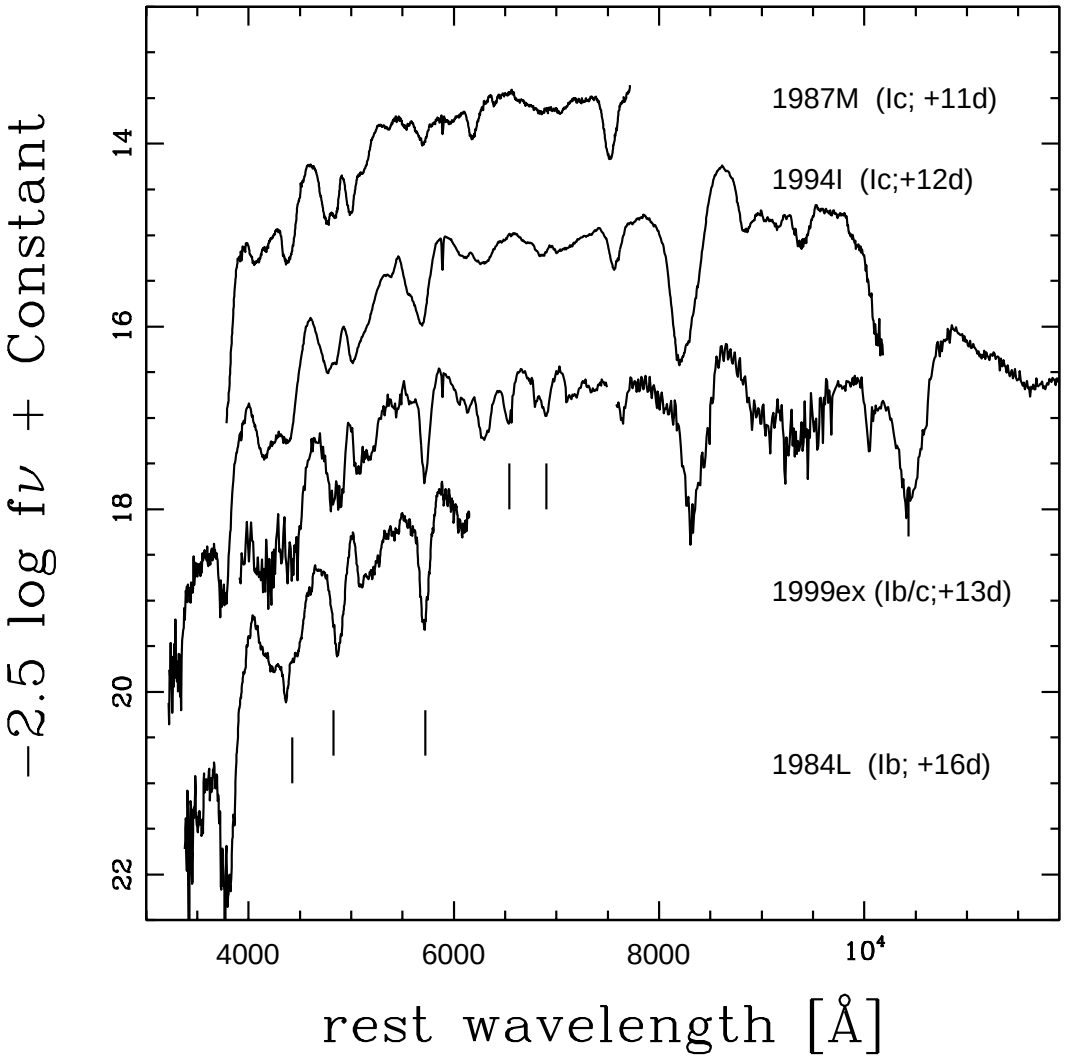

Fig. 11.— Same comparison as Figure 10, but for spectra taken two weeks past maximum.

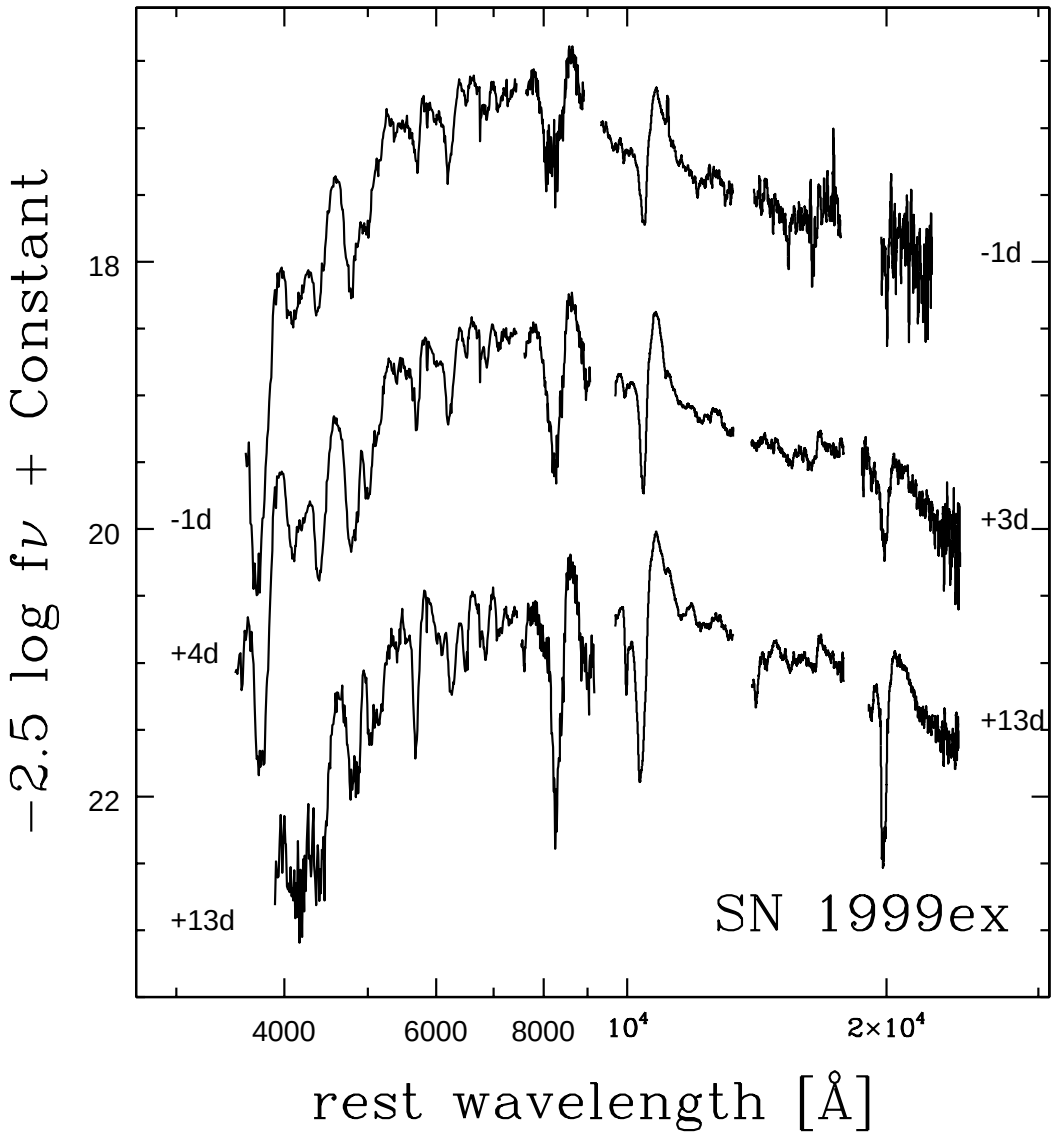

Fig. 12.— Combined optical and IR spectra of SN 1999ex in AB magnitudes. Days since B maximum are indicated next to each spectrum.

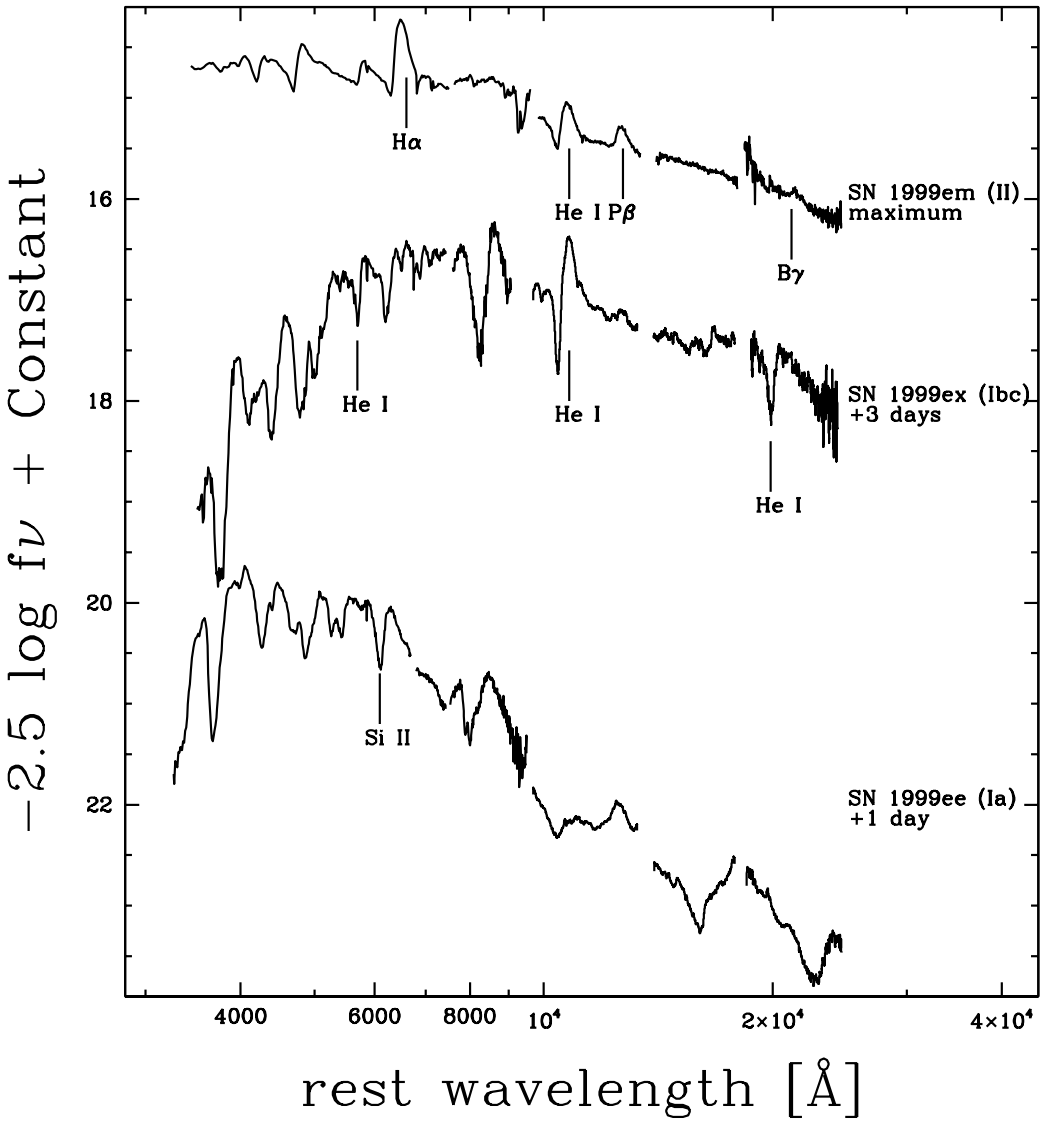

Fig. 13.— Combined optical and IR maximum-light spectra of the Type II SN 1999em, the Type Ib/c SN 1999ex, and the Type Ia SN 1999ee.